nature portfolio

Peer Review File

Molecular mechanism on forcible ejection of ATPase inhibitory factor 1 from mitochondrial ATP synthase

REVIEWER COMMENTS

Reviewer #1 (Remarks to the Author):

The manuscript "Molecular mechanism on forcible ejection of ATPase inhibitory factor 1 from mitochondrial ATP synthase" by Kobayashi et al. reports new and interesting findings concerning the interactions of regulatory protein IF1 and F1-subcomplex of bovine mitochondrial ATP synthase. The authors used proteins heterologically expressed in Escherichia coli. The ATPase activity of F1-subcomplex was measured both by biochemical methods and by single-molecule assay when it was immobilized on a glass and a bead was attached to subunit gamma, so that in responce to addition of ATP the authors could directly observe bead rotation. The latter method is a very powerful technique that allows to analyze enzyme activity and it regulation in molecular details.

The authors found that IF1 is a very efficient inhibitor of F1 ATPase activity. At temperature of 23C it bound to F1 with a time constant of 20 s at ATP concentration of 1 mM. This finding suggests that IF1 might promptly block ATP hydrolysis by FoF1 in mitochondria under de-energized conditions. The authors also demonstrated that IF1-inhibited F1 can be re-activated by forced rotation of subunit gamma in the ATP synthesis direction, but not in the hydrolysis direction. This is a new and important finding; previous studies of two other common regulatory mechanisms of bacterial F1 (ADP-inhibition and subunit epsilon) demonstrated activation in response to forced rotation in both directions. Finally, by using mutated variants of IF1 (with N-terminal truncations of 7, 12, 19, and 22 amino acid residues) the authors established that the interaction of N-terminal region of IF1 with subunit gamma is important for stabilization of the IF1-inihbited state of F1.

The manuscript is well-written in good English, the logic is clear, the methods are described in sufficient details, and the results support the conclusions. I think the manuscript can be published in Nature Communicatons after solving some issues described below.

1. All the experiments were done at 23C, while the physiological temperature for a cow is about 37C; at 23C body temperature a cow is kind of dead. It is clear that repeating the single-molecule experiments at 37C is not an option (lots of work + technically chllenging), but it is possible to repeat the biochemical activity measurements and the effects of IF1 at 37C. ATP synthase regulatory mechanisms are known to be temperature-dependent, so demonstrating that 23C and 37C experiments provide qualitatively similar results it important.

2.It was shown for Bacillus PS3 F1 (Ref. 34) that activation by forced rotation from ADP-inihibited state and from epsilon-inhibited state requires more energy than ATP synthesis. Is it possible to estimate, whether this is also the case with IF1 inhibition of bovine F1? This is a very important issue, because it affects the pattern of activation in whole mitochondria, where many copies of ATP synthase share the same coupling membrane. It might also explain why some research groups observed the decrease in ATP synthesis rate upon IF1 association to FoF1.

3. It is stated in the text (lines 179-181) that some molecules were excluded from the analysis. Since single-molecule assays provide the researcher with an option to choose "good" molecules and ignore

"bad" ones, it would be nice to include a table (in Supporting materials) that provides some statistics, e.g. how many molecules were in the viewfield of the microscope, how many of them were totally inactive, how many of the active ones were later rejected from the analysis.

4. The authors provide time constants for rotation phase and inhibition phase. However, for a biochemist it is more important to know, what percentage of time F1 was active, and what percentage of time it was inactive. (It can be calculated from the time constants, but it is not quite simple). I suggest that the infromation on the fractions of time that the enzyme was active/inactive should be added to the results section

Minor points:

Line 34 - "counterclockwise" is ambiguous, until the reader knows from which side we are looking

Line 40 - "rotated" is kind of confusing here, because rotation is generally associated with the rotor rotation. May be use the term "swing-out motion" as in line 278?

Line 46 - ATP synthesis is the primary role of FoF1 in mitochondria, but not in many bacteria. Better to specify it.

Line 53 - I have not seen any data direct on the effect of pmf on IF1 association. In bovine mitochondria pH is a crucial factor that controlls IF1 association, and I strongly recommend to add this fact to the Introduction. Acidification of the matrix usually results from anoxia and is accompanied by the drop in pmf, but it is difficult to prove the causal link between pmf and IF1 association.

Line 140 - what was the concentration of ATP?

Line 268 - the authors demonstrated that Pi also increases the probability of IF1 release upon gamma rotation, so ADP is not critically important for that. The discussion should be corrected accordingly.

Lines 342-347 - I think that the data on alanine substitutions are interesting and informative; may be include them in the results section?

Finally, citing some recent reviews on the regulatory mechanisms of ATP synthase might also improve the manuscript.

A PDF file with most of the comments above and with a few typos marked is also attached.

Conclusion: it is a well presented, laborious, elegant, and accurate experimental work. It will certaingly be of interest to researchers in the fields of biochemistry, biophysics, bioenergetics, cell biology, and physiology.

Reviewer #2 (Remarks to the Author):

The manuscript demonstrates the mechanism of release of the inhibitor IF1 from ATP-synthase, using magnetic tweezers to mimic and assist ATP synthesis. Technically it is exemplary, the conclusions are demonstrated beautifully, clearly, and beyond doubt using a method that while not novel remains extremely challenging. I am not qualified to judge the significance of the result to the field of inhibitory control of ATP synthase. From the perspective of single-molecule biology, it is of great interest to a general reader as an example of the use of single molecule methods to reveal mechanistic details in biological molecular machines.

Reviewer #3 (Remarks to the Author):

This study reports single-molecule manipulation experiments with immobilized bovine F1 linked to magnetic beads to elucidate the molecular mechanism of F1 inhibition by its natural inhibitory peptide IF1. The results showed that IF1-inhibited F1 was efficiently activated only when F1 was forcibly rotated (with magnetic tweezers) in the clockwise (ATP synthesis) direction, but not in the counter-clockwise direction (ATP hydrolysis), and the activation was enhanced in the presence of ADP and Pi. These observations suggest that the principal mechanism for the pmf-induced activation of IF1-inhibited FoF1 (in membranes) is the ejection of IF1 from F1 by pmf-driven Fo motor rotation. The results obtained with IF1 mutants strongly support a model in which the inhibitory effect of IF1 is mainly due the prevention of subunit beta conformational changes rather than changes in the interactions of IF1 with subunit gamma. These are major findings that provide novel and important insights into the mechanisms that regulate the activity of F1FO complexes. The presentation of the work is excellent.

I have only a few minor points:

-In the introduction (lines 52, 53), the authors may want to include a previous reference (Lefebvre-Legendre et al. Mol. Microbiol 2003) showing that F1-mediated ATP hydrolysis is essential for cell viability, for instance in cells of Saccharomyces cerevisiae lacking functional mitochondrial DNA (and hence the FO) where this activity is absolutely needed to maintain a sufficient mitochondrial membrane potential by the ADP/ATP translocase. In these pure ATP hydrolysis conditions, inhibition of F1 by IF1 would be lethal rising the possibility that IF1 does not necessarily bind to the F1 when it cannot dock to FO?

-The formulation “activation of IF1 inhibition” used all along the manuscript to indicate that F1 inhibition by IF1 is released is a bit confusing because it suggests instead that F1 becomes inhibited by IF1.

-line 79. Remove the ‘it’ before F1.

Molecular mechanism on forcible ejection of ATPase inhibitory factor 1 from mitochondrial ATP synthase

Ryohei Kobayashi[a,b], Hiroshi Ueno[a], Kei-ichi Okazaki[b,c], Hiroyuki Noji[a,*]

[a] *Department of Applied Chemistry, Graduate School of Engineering, The University of Tokyo, Hongo, Tokyo 113-8656, Japan*

[b] *Research Center for Computational Science, Institute for Molecular Science, Okazaki, Aichi 444-8585, Japan*

[c] *The Graduate University for Advanced Studies, Sokendai, Okazaki, Aichi 444-8585, Japan*

*Corresponding author: Hiroyuki Noji

Phone number: +81-3-5841-7252

Email: hnoji@g.ecc.u-tokyo.ac.jp

Abstract

IF_1 is a natural inhibitor protein for mitochondrial F_oF_1 ATP synthase that blocks catalysis and rotation of the F_1 by deeply inserting the N-terminal helices into F_1. A unique feature of IF_1 is the condition-dependent inhibition; although IF_1 inhibits the ATP hydrolysis of F_1, IF_1 inhibition is relieved under ATP synthesis conditions. To elucidate the condition-dependent inhibition mechanism, we performed single-molecule manipulation experiments on IF_1-inhibited *bovine* mitochondrial F_1 (bMF_1). The results showed that IF_1-inhibited F_1 was efficiently activated only when F_1 was rotated in the clockwise (ATP synthesis) direction, but not in the counter-clockwise direction. The observed rotational-direction-dependent activation explains the condition-dependent mechanism of IF_1 inhibition. Investigation of mutant IF_1 with the N-terminal truncation showed that the interaction with the γ subunit at the N-terminal regions is crucial for rotational-direction-dependent ejection, and the middle long helix is responsible for the inhibition of F_1.

Keywords:

ATPase inhibitory factor 1, IF_1, F_1-ATPase, Single-molecule manipulation, ATP synthase, F_oF_1

Introduction

F_oF_1-ATP synthase (F_oF_1) is a rotary motor protein that catalyzes ATP synthesis reaction from ADP and inorganic phosphate (P_i) using the proton motive force (*pmf*) across membranes. F_oF_1 is composed of two rotary motor proteins: F_o and F_1 [1–5]. F_o is a membrane-embedded protein complex forming the proton translocation pathway. When F_oF_1 synthesizes ATP, F_o transports protons from the outside to the inside of the membrane, accompanied by the clockwise rotation of the rotor complex inside F_oF_1 when viewed from the outside of the membrane. F_1 is a water-soluble portion of F_oF_1 that contains catalytic centers for ATP synthesis. Proton translocation by F_o and ATP synthesis/hydrolysis reactions in F_1 are tightly coupled through the rotation of the rotor complex. When *pmf* is sufficiently high, F_o forcibly rotates F_1, powered by proton translocation down *pmf*, resulting in ATP synthesis via F_1. When *pmf* is insufficient, F_1 reverses the rotation and hydrolyzes ATP, which induces F_o to pump protons to generate *pmf* [6].

F_1 is an ATPase that hydrolyzes ATP to rotate its rotor part counterclockwise against the surrounding stator $\alpha_3\beta_3$-ring [7], where the central rotor γ subunit is accommodated in the central cavity [8–12]. F_1 possesses three catalytic sites for ATP hydrolysis/synthesis, each at the interface between the α and β subunits. Amino acid residues critical for catalysis are mainly located in the β subunit. The "ground-state" crystal structure of *b*MF_1 [13] revealed that the three β subunits have different conformations and nucleotide-bound states; β with nucleotide analog (β_{TP}), β with ADP (β_{DP}), and β with none (β_E). The β_{TP} and β_{DP} adopt a closed form with their C-terminal domain rotated towards the γ-subunit, whereas β_E adopts an open conformation [4,12,14]. The rotary dynamics of F_1 have been investigated extensively using single-molecule studies [1,15–19]. The reaction scheme of rotary catalysis in *b*MF_1 [20] (Fig. 1A) was proposed by considering the structural features of *b*MF_1 and kinetic analysis in single-molecule studies on F_1 from thermophilic Bacillus PS3 (TF_1) [21]. Several experiments have shown that most of the crystal structures of *b*MF_1 represent catalytic dwell states [22–24].

F_oF_1 plays the primary role in ATP synthesis *in vivo*. ATP hydrolysis activity of F_1 can result in futile ATP consumption. Therefore, several types of regulatory systems can suppress or block the ATP hydrolysis activity of F_1 [25–28]. The most common mechanism universally found in bacterial and mammalian F_1 is ADP inhibition in which F_1 spontaneously lapses into a resting state during rotation [29–31]. Mitochondrial F_1s have a unique inhibitor protein, termed the ATPase inhibitory factor 1 (IF_1) [32]. It is found in eukaryotic cells and highly conserved particularly among mammalian cells [25]. Unlike the ε subunit [9,33–36] that some of the bacterial F_1s employ for inhibition, IF_1 is not a built-in inhibitor, but a dissociative one that associates with F_1 when the *pmf* is low or F_1 is not docked to F_o [6]. The most remarkable feature of IF_1 is its condition-dependent manner of inhibition: IF_1 inhibits ATP hydrolysis activity of F_1 almost completely under ATP hydrolysis conditions, whereas, in ATP synthesis conditions, IF_1 dissociates from F_1 and does not interfere with ATP synthesis reactions after

dissociation [32,37]. Notably, a few recent studies claim that IF_1 also suppresses the rate of ATP synthesis when IF_1 is overexpressed in cells [38,39].

The atomic details of the interaction between IF_1 and bMF_1 have been investigated in structural studies [40–42]. Full-length bovine mitochondrial IF_1 forms a homodimer complex via an antiparallel coiled coil [43], which associates two molecules of the F_1-ATPase with each N-terminal region, whereas the C-terminal region of IF_1 forms a coiled-coil structure for dimerization [40]. Deletion of the C-terminal residues 61–84 produces a stable monomeric form of IF_1 without the loss of inhibitory activity [44], which is often used in biochemical [45,46] and structural studies [41,42], including this study. The crystal structure of the bMF_1-IF_1 complex [42] showed that the long α-helical structure in the middle section of IF_1 was bound to the interface of the $\alpha\beta_{DP}$ pair, whereas the short helix of the N-terminus was in contact with the γ subunit. The N-terminal short helix was linked to the middle-long helix via a distinct kink (Fig. 1B). The crystal structure of bMF_1 with three IF_1 units, referred to as bMF_1-$(IF_1)_3$, has been resolved [41], where each αβ interface was bound with IF_1. Because the structures of the αβ interface are different, IF_1's show different conformational states. The structure of IF_1 on $\alpha\beta_{DP}$ is consistent with that of the 1:1 bMF_1-IF_1 complex, whereas the N-terminal short helix of IF_1 is not resolved on $\alpha\beta_{TP}$. The structure of IF_1 on $\alpha\beta_E$ shows the second half of a long helix, and the remaining was unsolved. Based on these observations, the progressive folding of IF_1 coupled with γ rotation has been proposed. Progressive folding process has also been suggested in biochemical studies [46,47], although the progressive processes are simplified as a two-step process: the initial binding process and the subsequent isomerization process.

Compared to studies under hydrolysis conditions [46,48,49], studies on IF_1 under synthetic conditions are less advanced, despite its importance for the understanding of the condition-dependent inhibition mechanism of IF_1. IF_1-inhibited state of F_1-ATPase is known to be so stable that ~~it~~ F_1 is unable to eject IF_1 by thermal agitation alone[46]. A typical condition for the unlocking from IF_1 inhibition is to charge sufficiently high *pmf* to membrane vesicles containing IF_1-inhibited F_oF_1 [50–55]. However, the principal mechanism for activation from IF_1 inhibition remains elusive, and many fundamental questions are unsolved such as 'Does reversible rotation lead to activation from IF_1 inhibition?', 'Are there factors to enhance the activation?', and 'Which interactions among IF_1 and F_1 are responsible for IF_1 inhibition and for condition-dependent inhibition?'

This study investigates the experimental conditions required for the IF_1 dissociation from inhibition complex using magnetic tweezers, which enables control of the angular orientation of the rotor during the single-molecule rotation assay for bMF_1 (Fig. 1C). Similar to the mechanical activation of F_1 from the ADP inhibited form, we forcibly rotated the rotor of IF_1-inhibited F_1, and defined activation as the resumption of F_1 molecule rotation. The activation probability was determined as a function of the angle, similar to our previous stall-and-release experiments [20,21,31,56]. Further, we investigated the roles of the N-terminal short helix and the middle-long helix in inhibition

and activation. These results highlight the molecular mechanism of IF_1 dissociation, which is critical for the unidirectional inhibition mechanism of IF_1.

Results

IF_1-inhibited states of bMF_1

The rotation of *b*MF_1 was monitored using magnetic beads (φ ~300 nm) attached to the γ subunit as a rotation probe and recorded at 30 frames per second (fps). During rotation, *b*MF_1 showed a transient pause in the absence of IF_1 [20]. This was attributed to ADP inhibition. Fig. S1 summarizes the kinetic analyses of ADP inhibition. Although it is dependent on ATP concentrations, the mean time for ADP inhibition range between 10-[illegible]s. For IF_1 inhibition, monomeric bovine IF_1 (Δ61–84) was used, as described in previous studies [45,46].

The experimental procedure for the analysis and manipulation of IF_1-inhibited *b*MF_1 molecules was as follows (Fig. 2A); after identification of rotating particles in the presence of 1 mM Mg-ATP, a solution containing IF_1 and Mg-ATP was gently introduced into the flow cell. After rotations for several tens of seconds, all *b*MF_1 molecules stopped rotation without exception (Fig. 2B), and none of the observed molecules resumed rotation during the observation time of 480 s (Fig. S2A). The pause duration was evidently longer than the duration of ADP inhibition, and thus attributed to IF_1 inhibition. Under 3 μM IF_1 and 1 mM ATP, the mean time to lapse into IF_1 inhibition was approximately 20 s (Fig. S2B). The time constant for IF_1 inhibition obtained in our biochemical experiments at saturated ATP and IF_1 concentrations (Fig. S9, gray) was 30 s, which is approximately 1.5 times longer than that in the single-molecule rotation assay. This is probably due to differences in experimental conditions; the single-molecule rotation assay selectively analyzes actively rotating molecules, whereas biochemical measurement is based on ensemble averaging of active and ADP-inhibited molecules. The latter would require a longer time to lapse into IF_1 inhibition than actively rotating molecules when ADP inhibited from is off the pathway to IF_1 inhibition.

Next, we investigated the dwell position of *b*MF_1 when inhibited by IF_1. Experiments were performed under 100 nM ATP condition, where *b*MF_1 showed three distinct pauses at the ATP-binding dwell angles (Fig. 2C). Transient pauses, such as ADP inhibition, are rarely observed [20]. When a solution containing 100 nM ATP and 5 μM IF_1 was introduced into the flow chamber, *b*MF_1 stopped rotating completely. The time constant for IF_1 inhibition at 100 nM ATP was 461 s (Fig. S3), which was longer than that obtained with 1 mM ATP, i.e., 19.6 s (Fig. S2B). The observed ATP-dependent effect of IF_1 inhibition was consistent with previous biochemical analysis [46,47,57,58]. Fig. 2C shows a representative dataset for the angular position analysis of IF_1 inhibition. The angular position of IF_1 inhibition was determined using the ATP-binding dwell angles as the reference (Fig. 2C, blue); it was defined as the angular distance from the left-side ATP-binding pause (Fig. 2C, pink). The position of IF_1 inhibition was determined as 89 ± 14° from the ATP-binding angle. This value was almost identical to the pause positions of *b*MF_1 stalled by AMP-PNP (76°) [20] and sodium azide (79°, Fig. S4), which

corresponds to the position of the catalytic dwell (80°). Thus, we confirmed that IF_1-inhibited *b*MF_1 pauses at the catalytic dwell angle, as seen in human mitochondrial F_1 [19].

Activation of IF_1-inhibited bMF_1 via forcible rotation

In the rotation assays, IF_1-inhibited *b*MF_1 did not resume the rotations once it lapsed into IF_1 inhibition. By contrast, it was reported that F_oF_1 is activated from IF_1 inhibition when the *pmf* is charged on the vesicle membrane, in which the F_oF_1 is embedded [53]. To explore the crucial conditions and factors for unlock from IF_1 inhibition, IF_1-inhibited *b*MF_1 molecules were forcibly rotated using magnetic tweezers. First, we tested the clockwise rotation for one turn (Fig. 3A), considering that forcible rotation in the ATP synthesis direction for one turn is sufficient for the unlock from IF_1 inhibition. Before the forcible rotation, the buffer in a flow cell was exchanged with IF_1-free ATP solution to prevent possible rebinding of IF_1. However, the molecules did not show activation in most cases; after released from magnetic tweezers, most of molecules just returned to the original position to continue the IF_1 pause (Fig. 3B). Only small fraction of molecules (10%) resumed continuous rotation. When forcibly rotated in counterclockwise direction, the activation probability was even lower (<4%), suggesting the rotational-direction-dependency for the activation from the IF_1 inhibition. The reactivation is a unique phenomenon that was never observed without manipulation with magnetic tweezers, but the probability is too low compared to the reported *pmf*-induced full activation of F_oF_1 [50–55].

Next, we tested the effect of ADP and P_i in a forcible rotation to further mimic ATP synthesis conditions. After confirming IF_1 inhibition, the buffer in the flow cell was gently exchanged with IF_1-free ATP synthesis buffer (100 μM ATP, 100 μM ADP, 1 mM P_i), and then, IF_1-inhibited *b*MF_1 molecules were forcibly rotated in the clockwise or counterclockwise direction for 360°. As shown in Fig. 3B, a remarkable increase in activation was observed when IF_1-inhibited *b*MF_1 was rotated in clockwise direction in the presence of ADP and P_i; the probability of activation was about 60%. This is in contrast to the reactivation probability for clockwise manipulation in ADP/P_i-free solution (10%). Evident rotational-direction-dependent manner was observed; the counterclockwise rotation failed the activation. These observations indicate that both directional manipulation and the presence of substrates for ATP synthesis are requisite for the efficient activation of the IF_1-inhibited state. To investigate the effect of individual substrates on activation, we performed the same manipulation experiment in the presence of ADP or P_i, respectively (Fig. S5). P_i was more effective for reactivation (28%), whereas the activation achieved only 4% in the presence of ADP. Notably, once activated, *b*MF_1 molecules did not show long pauses that are attributable to IF_1 inhibition in IF_1-free solution. This observation indicates that activation is accompanied by dissociation of IF_1 from F_1.

Angle-dependence of IF_1 dissociation

We determined the activation probability as a function of the rotation angle by performing a "stall-and-release" experiment. The experimental procedure was as follows (Fig. 4A); after confirming IF_1 inhibition, the inhibited *b*MF_1 molecules were rotated to stall at the target angle for the programmed period of 0.5–5.0 s with the magnetic tweezers. After the set time had elapsed, the magnetic tweezers were turned off to release the F_1 molecule. The released molecule showed two types of behaviors (Fig. 4B): starting active rotation or returning to the initial position of IF_1 inhibition to resume the pause. The former behavior was identified as activation from IF_1 inhibition, and the latter as false of activation. In contrast to the abovementioned activation by a forcible 360° rotation, we conducted a stall-and-release experiment without washing IF_1 in solution. The molecules again lapsed into IF_1 inhibition after activation due to the rebinding of IF_1 in a solution containing 3 μM IF_1. The mean rotation time until the re-inactivation of activated F_1 molecules was 1[illegible]s (Fig. S6), and the result is consistent with the time constant of IF_1 inhibition (15.2 s), indicating that re-inactivation was due to the rebinding of IF_1 from solution. We repeated the manipulation of each molecule to confirm reproducibility. After manipulation, a few molecules occasionally exhibited unusual behaviors, such as random tethered Brownian motion, and nonspecific binding to or detachment from the coverslip. These data were omitted from the analyses. A detailed description of the analysis of molecules in this experiment is presented in Fig. S7 and Methods.

Experiments were conducted with 100 μM ATP, 100 μM ADP, and 1 mM P_i. Fig. 4C shows the experimental results, where the counterclockwise direction of the stall angle was defined as positive relative to the initial IF_1-inhibited state. In principle, activation was rarely observed in the counterclockwise manipulation, which is consistent with the experimental results for forcible 360° rotation manipulation (Fig. 3B). For clockwise manipulation, rotation up to 120° did not activate IF_1-inhibited *b*MF_1. When rotated over 200°, the activation probability, i.e., P_{ON} was remarkably increased. P_{ON} was 60% when stalled at -200° for 2 s, and reached over 90% when stalled at –320° for 5 s. At each stall angle, P_{ON} increased with stall times. These features are similar to those observed in our previous studies on the angle dependence of ATP binding and hydrolysis in TF_1 [56] and *b*MF_1 [20] as well as the angle dependence of activation from ADP inhibition [30]. These results on angle-dependent activation are discussed in detail in the Discussion section.

N-terminal-truncated mutants of IF_1

With aim to investigate which structural elements of IF_1 are responsible for the observed rotation-direction-dependent activation, we generated IF_1 mutants with N-terminal truncations and tested their inhibitory functions in biochemical and single-molecule manipulation experiments (Fig. 5). IF_1 consists of the N-terminal region that is missing in the crystal structure (1–7), unstructured region (8–13), the short helix region (14–18), glycine loop (19–20), and the long helix region (21–60) (Fig. 5A, 5B). The long helix of IF_1 mainly interacts with the β_{DP} subunit, whereas the proximity

contacts with the γ subunit are found at S11 and F22 (Fig. 5A) [41]. We prepared four truncation mutants of IF_1: IF_1(Δ1–7), IF_1(Δ1–12), IF_1(Δ1–19), and IF_1(Δ1–22) (Fig. 5C). The inhibitory effects of the mutants were first analyzed using a solution ATPase assay (Fig. S8, S9). IF_1(Δ1–7) and IF_1(Δ1–12) showed similar inhibitory effects to wild-type IF_1; upon association with bMF_1, the mutants of IF_1 completely inhibited ATPase activity. In contrast, IF_1(Δ1–19) and IF_1(Δ1–22) showed a reduced inhibitory effect. At concentrations lower than 0.5 μM, IF_1(Δ1–19) did not completely inhibit ATPase activity, suggesting a reversible association/dissociation. IF_1(Δ1–22) showed a lower inhibitory effect with a peculiar kinetic behavior. Upon addition of IF_1(Δ1–22) into the assay mixture, ATPase activity decreased, followed by slow recovery. Although the mechanisms underlying such complex behavior are unclear, these biochemical measurements showed that the inhibitory effect of IF_1(Δ1–19) and IF_1(Δ1–22) was less than that of IF_1(Δ1–7) and IF_1(Δ1–12).

We analyzed the rotation of bMF_1 in the presence of truncated mutants of IF_1. Similar to the biochemical experiments, we observed that IF_1(Δ1–7) and IF_1(Δ1–12) showed nearly the same properties as those of IF_1(WT) (Fig. S10). As shown in the time-course and pause time analysis, inhibition by these mutants was essentially irreversible; IF_1-inhibited bMF_1 did not spontaneously resume active rotations within the observation time. In contrast, further N-terminal truncation had a significant effect on IF_1 inhibition. With IF_1(Δ1–19) and IF_1(Δ1–22), bMF_1 molecules did not completely stop the rotation, but the molecules showed frequent transitions between rotation and intervening pauses (Fig. S10J, S10M). The mean duration of pauses with IF_1(Δ1–19) or IF_1(Δ1–22) was 250 s or 60 s, respectively. These observations show that the short helix and N-terminus of the long helix of IF_1 have critical roles for the stabilization of IF_1 inhibition.

Rotation-direction-dependent activation was investigated with the mutant IF_1's. Whereas the activation experiments for IF_1(Δ1–7) and IF_1(Δ1–12) were conducted in IF_1-free solutions, those were done in the presence of IF_1 for IF_1(Δ1–19) and IF_1(Δ1–22). This is because these mutants can dissociate from F_1 during buffer exchange, hampering the activation experiment. Fig. 5D and 5E show the activation probabilities after a forcible 360° rotation in the counterclockwise and clockwise directions, respectively. The probabilities of activation from inhibition with IF_1(Δ1–7) and IF_1(Δ1–12) showed similar trends to that of IF_1(WT) in both directions; i.e., no activation after counterclockwise rotation, whereas clockwise rotation induced activation with a significant probability of 80%, which is higher than that for IF_1(WT) at 58%. These results indicate that the unstructured N-terminal region from positions 1 to 13 of IF_1 is not responsible for the principal mechanism of IF_1 inhibition, although the region contributes to the structural stabilization of the bMF_1-IF_1 complex. Unlike the truncation of the unstructured N-terminal region, the truncation of the short helix and the subsequent N-terminal region of the long helix had distinctive impact on rotation-direction-dependent activation. For the mutants IF_1(Δ1–19) and IF_1(Δ1–22), the activation probabilities after clockwise or counterclockwise rotation were both higher than those for IF_1(WT),

238 IF_1(Δ1–7), and IF_1(Δ1–12). In particular, a significant fraction of events showed activation after
239 counterclockwise rotation: 13% for IF_1(Δ1–19) and 80% for IF_1(Δ1–22). The activation probability
240 after clockwise rotation was also higher than that for IF_1(WT), IF_1(Δ1–7), and IF_1(Δ1–12), and was
241 close to 100%. These results suggest that IF_1 readily dissociates from *b*MF_1 without the short helix
242 and the N-terminal tip of the long helix, as suggested by biochemical data. Importantly, IF_1(Δ1–22)
243 almost loses the rotation-direction-dependent feature, and the activation probabilities after clockwise
244 or counterclockwise rotation are more than 80%. Considering that IF_1 shows direct contact with the γ
245 subunit in the truncated regions, these results suggest that the rotation-direction-dependent
246 dissociation mechanism is based on contact with the γ subunit. One may consider that IF_1(Δ1–22)
247 dissociates from *b*MF_1 not by forcible rotation, but by its nature of spontaneous dissociation. However,
248 the manipulation time is 2 s which is too short for spontaneous dissociation of IF_1(Δ1-22); the
249 probability of spontaneous dissociation within 2 s is only 3% when estimated from the mean time
250 constant of spontaneous activation, 60 s (see Methods). Thus, the observed activation with IF_1(Δ1–
251 22) results due to forcible rotation.

Discussion

In this study, we observed the activation of IF_1 inhibition by forcible rotation with magnetic tweezers. Activation is accompanied by the ejection of bound IF_1 from *b*MF_1. This is supported by the following observations: re-inactivation by IF_1 was observed only when the solution contained IF_1. In the absence of IF_1, the activated molecules did not show long pauses attributable to IF_1 inhibition. Second, the mean rotation time before re-inactivation was in good agreement with that for IF_1 inhibition (Fig. S6). The analysis of activation from IF_1 inhibition provides important implications for the mechanism of IF_1 inhibition. *b*MF_1 molecules during IF_1 inhibition were activated when the γ subunit was forcibly rotated with magnetic tweezers for over 200° in the clockwise (synthesis) direction. The activation probability was significantly enhanced when ADP and P_i were present in the solution. Thus, it is evident that reactivation of IF_1 inhibition occurs under ATP synthesis conditions. With IF_1(WT), the probability of activation reached 100% when stalled at –320° for 5 s. This is sufficiently high to explain the *pmf*-induced activation of the IF_1-inhibited F_oF_1 [50–55]. Thus, the principal mechanism for the *pmf*-induced activation of IF_1-inhibited F_oF_1 is the ejection of IF_1 from F_1 by forcible rotation powered by *pmf*-driven F_o motor in the F_oF_1 complex. The requirement of ADP and P_i for efficient activation indicates that forcible clockwise rotation should be coupled with the ATP synthesis reaction for IF_1 ejection. As the presence of substrates enhances the cooperative nature of F_1, IF_1 may likely be ejected through a concerted conformational transition of the α and β subunits coupled with γ subunit rotation.

We observed a significant increase in the probability of activation when the IF_1-inhibited *b*MF_1 was rotated over –200°. The crystal structure of *b*MF_1-IF_1 complex show that IF_1 binds to β_{DP} which represents the +200° state from the ATP-binding state (0°) in the scheme. These results suggest that IF_1 is ejected through the state transitions of the β subunit from the +200° state to the 0° state or –40° (Fig. 6A). This state transition should be coupled with the conformational transition of the β subunit from a closed to an open conformation. The closed-to-open transition accompanies the swing-out motion of the C-terminal domain of the β subunit to which IF_1 binds via the long α helix. Thus, IF_1 dissociates from the β subunit in an open conformation that facilitates IF_1 dissociation. The closed-to-open conformational transition would destabilize the *b*MF_1-IF_1 complex by pulling the N-terminal regions of IF_1 out of the γ subunit, because the C-terminal domain of the β subunit in the open conformation is apart from the axis of the γ subunit, compared with the closed conformation. This dissociation model is almost the reverse process of the IF_1 association proposed for the *b*MF_1-$(IF_1)_3$ structure, which suggests the progressive folding of IF_1 coupled with the conformational transition of the β subunit from β_E to β_{DP} via β_{TP}.

The above discussion indicates the reversible association/dissociation processes of IF_1. This can be viewed as an inevitable property for IF_1 to avoid being Maxwell's demon that violates the

second law of thermodynamics by allowing only one direction of motion in a microscopic system. If IF_1 can dissociate from F_1 without coupling with clockwise rotation, while IF_1 association is tightly coupled with counterclockwise rotation, the second law of thermodynamics will be violated as Maxwell's demon. This is evident when one considers the rotary motion of F_oF_1 under conditions where the torques of F_1 and F_o are balanced. In IF_1-free conditions, the rotor complex should show non-biased Brownian motion in both directions: clockwise and counterclockwise, in the F_oF_1 complex. Even though the rotor can cause occasional rotary steps in both directions, the mean rotational displacement does not increase. In contrast, in the presence of IF_1, F_1 should make a +200° rotation coupled upon the association of IF_1. This is because 'the tight coupling of IF_1 association and the rotation' means that IF_1 association induces +200° rotation. Although the pause by IF_1 inhibition should be long, IF_1 should eventually dissociates from F_1. Along the above assumption, IF_1 is dissociated without biasing rotation. Thus, each cycle of association and dissociation of IF_1 should cause the rotation by +200° in hydrolysis direction. After multiple events of IF_1 association and dissociation, F_1 undergoes unidirectionally biased rotation in hydrolysis direction. Thus, the assumption of the asymmetric coupling model should violate the second law of thermodynamics, and the reversibility of IF_1 association/dissociation seems inevitable. For the same reason, the requirement for ADP and P_i for IF_1 dissociation is also inevitable, considering that IF_1 association is coupled with ATP hydrolysis.

This consideration would be applicable to other regulatory systems of F_oF_1. In addition to IF_1, several types of inhibitory mechanisms can block the ATP hydrolysis. The ζ subunit of α-proteobacteria inhibits hydrolysis by binding to the interface of the $\alpha\beta_{DP}$ pair in a manner similar to IF_1 [59–61]. Mycobacteria have a specific insertion sequence at the C-terminal of the α subunit called the α-extension loop [62,63]. Recent cryo-EM analysis showed that the α-extension loop binds to a specific loop on the γ subunit, which is considered to block rotation in a counterclockwise direction [26,64]. When these inhibitory processes are coupled with the rotation of the γ subunit, the dissociation of the ζ subunit or the α-extension loop has to be coupled with rotation in the opposite direction, according to the above contention.

Structural analyses of the bMF$_1$-IF$_1$ complex showed that IF_1 has interactions with bMF$_1$ via two parts: an N-terminal region with an unstructured loop and a short helix (1–20), and a central long helix (21–60) (Fig. 5A and 5B). The major interaction between IF_1 and F_1 is formed by the central long helix, which is accommodated on the C-terminal domain of the β subunit. The N-terminal region of IF_1 wraps around the γ subunit, with evident contacts at S11 and F22 of IF_1. Accordingly, two scenarios for the principal mechanism of IF_1 inhibition are possible [40]. First is the mechanical hindrance of the γ subunit rotation by the N-terminal region of IF_1. The second model assumes the prevention of β conformational transitions by the central long helix of IF_1. The investigation of IF_1 mutants with N-terminal truncation provides important clues to this question. We observed that

IF_1(Δ1–19) and IF_1(Δ1–22) maintained inhibitory potency to halt the catalysis and rotation of *b*MF_1, although these mutants were remarkably less effective than IF_1(WT) or other mutants. IF_1(Δ1–22) was truncated before F22, losing all residues that were in contact or close proximity to the γ subunit. Thus, our study suggests that the interaction with the γ subunit is dispensable, supporting the latter model. Our result was also supported by the research using F_1 and IF_1 from yeast mitochondria: deletion of all the residues preceding F17 in yeast IF_1, corresponding F22 in bovine IF_1, still maintained the inhibitory capacity [65]. This result implies a universal IF_1 inhibition mechanism beyond the species level.

In the atomic structures of *b*MF_1-IF_1 and *b*MF_1-$(IF_1)_3$, hydrophobic residues in the central long helix, including Y33, form strong interactions with the C-terminal domain of the β subunit, providing most of the binding energy. The binding of IF_1 to F_1 is further augmented by salt-bridge formation between E30 in IF_1 and R408 in the β_{DP} subunit. The contribution of these residues was experimentally confirmed in mutagenetic approaches [45,46]. A possible molecular mechanism for IF_1 inhibition is that the tight binding of IF_1 with the β subunit prevents conformational transition requisite for rotary catalysis. There are several highly conserved charged residues in the C-terminus of IF_1, and the roles of these residues have not been clarified. As a preliminary trial, we conducted molecular dynamics simulation where the γ subunit is forcibly rotated in synthesis direction. The interaction between the positive charged of the γ subunit and negative charge of IF_1 was suggested, which is reminiscent of the ionic track [66]. Based on this observation, we tested the role of these conserved charged residues by selectively substituting five residues with alanine (Fig. S11 and S12). Except for a slight decrease in binding affinity to *b*MF_1, no clear differences were found between IF_1(WT) and the alanine-substitution mutant in the IF_1 inhibition assay as well as in manipulation assay. Our experiments suggest that C-terminal charged residues have little impact on the inhibitory mechanism and the rotation-direction-dependent dissociation.

Analyses of N-terminal truncation mutants revealed the molecular mechanism of rotary-direction-dependent dissociation of IF_1 from F_1 (Fig. 6B). IF_1(Δ1–22), which loses residues in contact with the γ subunit, showed a significantly high activation probability after the forcible rotation of 360°. The important finding in this mutant is that both of the clockwise and counterclockwise rotation resulted in the efficient activation of IF_1 inhibition with almost equal probability (Fig. 5D and 5E). This is in contrast to the asymmetric features of IF_1(WT), IF_1(Δ1–7), and IF_1(Δ1–12), which showed activation only via clockwise rotation. In the case of IF_1(Δ1–19), the asymmetric effect of forcible rotation was retained. However, a higher activation probability is observed. These observations indicate that the N-terminal region of the central long helix plays a crucial role in rotary-direction-dependent activation, and the N-terminal short helix also contributes to this result. The truncated residues in IF_1(Δ1–22), in addition to the 1–19 truncation, are G20, A21, and F22. Among them, F22 is bulky compared with the other residues. Further, in the crystal structures of the *b*MF_1-IF_1 complex,

360 F22 is in direct contact with I16 of the γ subunit. Considering these points, F22 is likely one of the
361 most critical residues for rotary-direction-dependent activation. Molecular dynamics simulations of
362 the *b*MF_1-IF_1 complex would provide more detailed information on the molecular mechanism of
363 rotation-direction-dependent activation.

Acknowledgments

We thank S. Mori (University of Tokyo) for technical advice, T. Sagawa (University of Tokyo) for critical discussions regarding theoretical aspects of Maxwell's demon concept, and all members of the Noji Laboratory for their valuable comments. This work was supported in part by a Grant-in-Aid for Scientific Research on Innovation Areas (JP19H05380 and JP21H00388 to H.U.), a Grant-in-Aid for Scientific Research (S; JP19H05624 to H.N.) from the Japan Society for the Promotion of Science, and a Research Grant from Human Science Frontier Program (Ref. No: RGP0054/2020 to H. N.).

Author Contributions

R. K., H. U., and H. N. designed the research; R. K. conducted all experiments and analyses; K.O performed molecular dynamic simulation; R. K. and H. N. wrote the paper with support from H.U. and K. O..

Competing of Interests

The authors declare no competing interests.

Methods

Purification of bMF_1 and IF_1

F_1-ATPase from bovine mitochondria with two mutated cysteine residues at A99 and S191 at the γ subunit and nine histidine residues (His-tag) at the N-terminus of the β subunit (hereafter referred to as bMF$_1$) was purified as described previously [20]. IF$_1^{1\text{-}60}$ with the linker and mScarlet fused to the C-terminus (referred to as IF$_1$(WT)), was purified as described previously [46]. The N-terminal truncated mutants and C-terminal alanine mutant of IF$_1$ were prepared as follows. Fragments of the N-terminal truncated mutants, deleted in the region encoding the corresponding N-terminal region, were generated by PCR, using sets of mutation primers. The sequence encoding the C-terminal alanine mutant was amplified by PCR using primers containing mutations. The resulting PCR products were subjected to gel electrophoresis and purification. The insert plasmid and vector IF$_1$(WT) plasmid were digested with the same restriction enzymes. The products were ligated and introduced into *Escherichia coli* JM109. The sequence of the recombinant IF$_1$ plasmid was confirmed using the Fasmac sequencing service (Fasmac, Japan). The purified mutant proteins were confirmed by SDS-PAGE and MALDI-TOF/TOF mass spectrometry (Genomine. Inc., Korea or IDEA Consultants, Inc., Japan) (Fig. S13, Table S1).

Solution experiment

The ATPase activity of bMF$_1$ was monitored as the rate of NADH oxidation [46]. The basal buffer contained 50 mM HEPES-KOH (pH 7.5), 50 mM KCl, 2 mM $MgCl_2$, and an ATP-regenerating system (0.2 mg/mL pyruvate kinase and 2.5 mM phosphoenolpyruvate) supplemented with 0.2 mM NADH and 50 μg/mL lactate dehydrogenase, as described previously [46]. Experiments were conducted at 25°C using a V-660 (JASCO, Tokyo, Japan) UV/VIS spectrophotometer equipped with a Peltier-type temperature controller (ETCS-761). ATP hydrolysis by bMF$_1$ was initiated by adding purified bMF$_1$ into the basal buffer with 1 mM ATP. For the reaction to reach a steady state, we waited for 180 s before IF$_1$ injection into the reaction mixture. After the IF$_1$ injection, the rate of ATPase activity changed. Inhibition by IF$_1$ was quantified by estimating the apparent rate constants for IF$_1$ ($k_{inhibition}^{app}$), which were determined by fitting the decay using the following equation:

$$y(t) - y_0 = V_\infty t + \frac{V_0 - V_\infty}{k_{inhibition}^{app}}\left\{1 - \exp\left(-k_{inhibition}^{app} t\right)\right\} \quad \text{(Eq. 1)}$$

where $y(t)$ and y_0 are the absorbance values at the time t and 0 after IF$_1$ injection to the solution cuvette, respectively, and V_0 and V_∞ are the initial and final rates of reaction, respectively. Fitting was performed using the time course of NADH absorbance at 2 s after IF$_1$ addition. Because exponential decay was not observed in the time course of IF$_1$(Δ1–22) inhibition (Fig. S8G), curve fitting using (Eq. 1) were not performed.

If the reaction was irreversible, as shown in IF_1 (WT), IF_1 (Δ1–7), and IF_1 (Δ1–12), the following reaction scheme may represent sequential IF_1 inhibition:

$$F_1 + IF_1 \underset{k_{off}}{\overset{k_{on}}{\rightleftarrows}} F_1 \cdot IF_1 \xrightarrow{k_{lock}} F_1 \cdot IF_1^{lock} \qquad \text{(Scheme 1)}$$

where $F_1 \cdot IF_1^{lock}$ represents the inactive state, and $F_1 \cdot IF_1$ is the intermediate state that is still catalytically active. k_{on} and k_{off} represent the rate constants of association and dissociation, respectively. k_{lock} is the rate constant of isomerization to the locked state. According to (Scheme 1), $k_{inhibition}^{app}$ can be expressed as follows:

$$k_{inhibition}^{app} = \frac{k_{lock}[IF_1]}{K_M^{IF_1} + [IF_1]} \qquad \text{(Eq. 2)}$$

$$K_M^{IF_1} \equiv \frac{k_{off} + k_{lock}}{k_{on}} \qquad \text{(Eq. 3)}$$

which shows a typical hyperbolic relationship.

Rotation assay of bMF1

For the rotation assay, *b*MF_1 was immobilized onto the glass surface, and magnetic beads were attached to the two cysteine residues of the γ subunit (γA99C and γS191C) through a biotin-avidin interaction. The protocol was as follows [20]. A flow chamber (~5 μL) was prepared with two coverslips (18 × 18 mm^2 at the top, and 24 × 32 mm^2 at the bottom; Matsunami Glass) with double-sided tape (7602 #25, Teraoka) as a spacer. Purified *b*MF_1 (~500 pM) in observation buffer (50 mM HEPES-KOH (pH 7.5), 50 mM KCl, and 2 mM $MgCl_2$) was gently introduced into the flow chamber and incubated for 5–10 min. After washing unbound *b*MF_1 with more than 50 μL of observation buffer containing ~10 mg/mL BSA, streptavidin-coated magnetic beads (GE Healthcare), which were pre-centrifuged to enable the use of relatively small beads (~300 nm), were introduced into the flow chamber. Unbound beads were washed with more than 50 μL of observation buffer containing the prescribed concentrations of ATP and/or ADP/P_i. Rotations of the magnetic beads were observed using a phase-contrast microscope (IX-70, Olympus) with a 100× objective lens at a recording rate of 30 fps. The rotation assay was performed at 23 ± 2 °C. The ATP-regenerating system (0.2 mg/mL pyruvate kinase and 2.5 mM phosphoenolpyruvate) was added to the solution mixture unless ADP was used.

To observe the IF_1 inhibitory state, we identified rotating molecules among the particles attached to the coverslip in the IF_1-free solution. Next, a solution containing IF_1 and ATP/ATP synthesis (100 μM ATP, 100 μM ADP, and 1 mM P_i) was infused into the flow chamber. After rotation, *b*MF_1 molecules eventually stopped rotation (Fig. 2A).

Manipulation with magnetic tweezers

Magnetic tweezers, comprising two sets of electromagnets, were equipped onto the microscope stage and controlled by custom-made software [20,56]. Rotations were imaged at 30 fps using a progressive-scan camera (FC300M, Takex, Kyoto, Japan), which enabled real-time manipulation using magnetic tweezers. Movies were stored on a computer as AVI files and analyzed using custom-made software.

Kinetic analysis of ADP inhibition

Rotations in the IF_1-free solution were recorded for > 10 min per molecule (Fig. S1). Under these conditions, ATP binding occurs for less than 1 ms, and therefore, cannot be detected as a pause of rotations with magnetic beads at a recording rate of 30 fps. However, *b*MF_1 showed frequent transient pauses; we collected the data from all pauses longer than 1 s [29] and rotary traces between pauses longer than 1 s were defined as rotations. The distribution of pausing times before starting rotations was fitted by a double exponential function, $y = N_{sp}\exp(-t/\tau_{sp}) + N_{lp}\exp(-t/\tau_{lp})$, where N_{sp} and N_{lp} are constants, and τ_{sp} and τ_{lp} are time constants for the short and long pause, respectively. A relatively short pause (sp) corresponds to decelerated P_i release, as previously reported [29,67]. Long pause (lp) corresponds to the ADP-inhibited form. These results showed that the timescale for ADP inhibition was 10-30 s under the various conditions tested. The distribution of rotating times before lapsing pauses was fitted by a single exponential function, $y = N_{rot}\exp(-t/\tau_{rot})$, where N_{rot} is a constant and τ_{rot} is a time constant for rotations.

Analysis of IF_1 inhibition

The experimental procedure was described in the main text (see also Fig. 2A). Rotating time (Fig. S2, S3, S6, S10, and S12) was defined as the period of time from the completion of solution exchange until when the molecules fell into IF_1 inhibition. Probability plots versus rotating time was fitted by a single-exponential decay function to estimate the mean rotation time, $\tau_{rot}^{IF_1}$. Pauses were defined as that longer than 1 s, observed in the solution containing IF_1. Except IF_1(Δ1–19) and IF_1(Δ1–22), most of the pauses showed extremely long pausing state over 480 s, corresponding to IF_1 inhibition. A few traces showed relatively short pausing state of ~20 s. They were attributable to ADP inhibition because the timescales of these pauses were mostly identical to that estimated from IF_1-free solution experiment (see Fig. S1). All of them spontaneously recovered active rotation and eventually fell into IF_1 inhibition without exception. For IF_1(Δ1–19) and IF_1(Δ1–22), rotations were frequently recovered without manipulation indicating a reversible inhibition/dissociation mechanism. The histogram of pausing time was fitted by single-exponential decay function for IF_1(Δ1–19) to estimate the mean duration time, $\tau_{pause}^{IF_1}$, 254 s. For IF_1(Δ1–22) analysis, the double-exponential decay function was applied to fit the histogram, estimating $\tau_{lp}^{IF_1}$ and $\tau_{sp}^{IF_1}$. Although the underlying

484 molecular mechanism corresponding to $\tau_{sp}^{IF_1}$ is unclear, we selected $\tau_{lp}^{IF_1}$ for IF_1(Δ1–22) inhibitory
485 states.
486
487 *Selection of molecules in the manipulation experiments*
488 To discriminate IF_1 inhibition from ADP inhibition, we adopted the following method in the
489 manipulation experiments. For forcible 360° manipulation experiment (Fig. 3, 5 and Fig. S5, S12), we
490 waited for 480 s after confirming a pause, because IF_1 inhibition was irreversible and did not recover
491 rotation within the observation period (Fig. S2A) whereas ADP inhibition was reversible and
492 spontaneously recovered rotation. In the "stall-and-release" experiment, we selectively analyzed the
493 molecule that showed activation by 360° clockwise rotation. Thus, the maximum probability shown
494 in the figures (*e.g.* Fig. 4C) was 100%, whereas around 60% in the forcible 360° manipulation where
495 all molecules are subject to analysis.
496 It is noted that the difference between IF_1 inhibition and ADP inhibition appeared in the
497 activation probability by counterclockwise manipulation, as well as the length of the pausing time.
498 Pauses observed in IF_1-free solution can be almost completely activated by the stall at +80° in the
499 counterclockwise direction for 2 or 5 s (Fig. S7, triangles). By contrast, IF_1 inhibition, which was
500 defined as the pauses longer than 480 s under saturating IF_1 conditions, was not activated by the same
501 manipulation (Fig. S7, squares). Thus, IF_1-inhibited state was confirmed by the following way; after
502 re-inactivation by IF_1 in solution, we stalled the targeted molecules at +80° in the clockwise direction
503 before each trial. We analyzed the molecule that did not show reactivation by the abovementioned
504 manipulation.
505 Through repeated manipulations with magnetic tweezers, molecules sometimes showed
506 unusual fluctuations. This may reflect the unstable states of the molecules or their detachment from
507 the coverslip. Such molecules cannot be reactivated by forcible 360° clockwise rotation.
508 Contamination of these molecules in the analysis lowers the probability of reactivation. We
509 concluded that reliable data cannot be obtained if such disordered molecules are subjected to further
510 experiments. For molecules that no longer resumed active rotation after 360° clockwise rotation, we
511 completed the manipulation of the molecules and searched for a new molecule.
512
513 *Probability of spontaneous reactivation during manipulation*
514 Unlike IF_1(WT), IF_1(Δ1–7) and IF_1(Δ1–12), IF_1(Δ1–19) and IF_1(Δ1–22) did not stop rotations
515 of *b*MF_1 completely. Considering the inherent pausing time of these two mutants, 250 s and 60 s,
516 respectively (Fig. S10), we selectively manipulated pausing states that last for longer than 100 s for
517 IF_1(Δ1–19) and 60 s IF_1(Δ1–22).
518 Inhibitory states by IF_1(Δ1–22) were reactivated by manipulation of 360° at the rate of 0.5
519 rps, that is, 2 s per manipulation. To exclude the possibility that rotations resumed irrespective of

manipulation for 2 s, we performed the following calculation. The mean pausing time by $IF_1(\Delta 1–22)$ was 60 s, whereas short pauses, lasting only 2 s on average, were also observed. As mentioned above, we waited for 60 s to selectively manipulate the long pauses after confirming the pauses. Thus, the impact of short pauses on this analysis was negligible. The probability that these pausing states end in 2 s is calculated using the following equation:

$$100 \times \frac{\int_0^2 \exp\left(-\frac{t}{60}\right) dt}{\int_0^\infty \exp\left(-\frac{t}{60}\right) dt} = 3\%$$

Therefore, the probability of simultaneous reactivation was so small that we concluded that the reactivation of rotation was invoked by the manipulation itself.

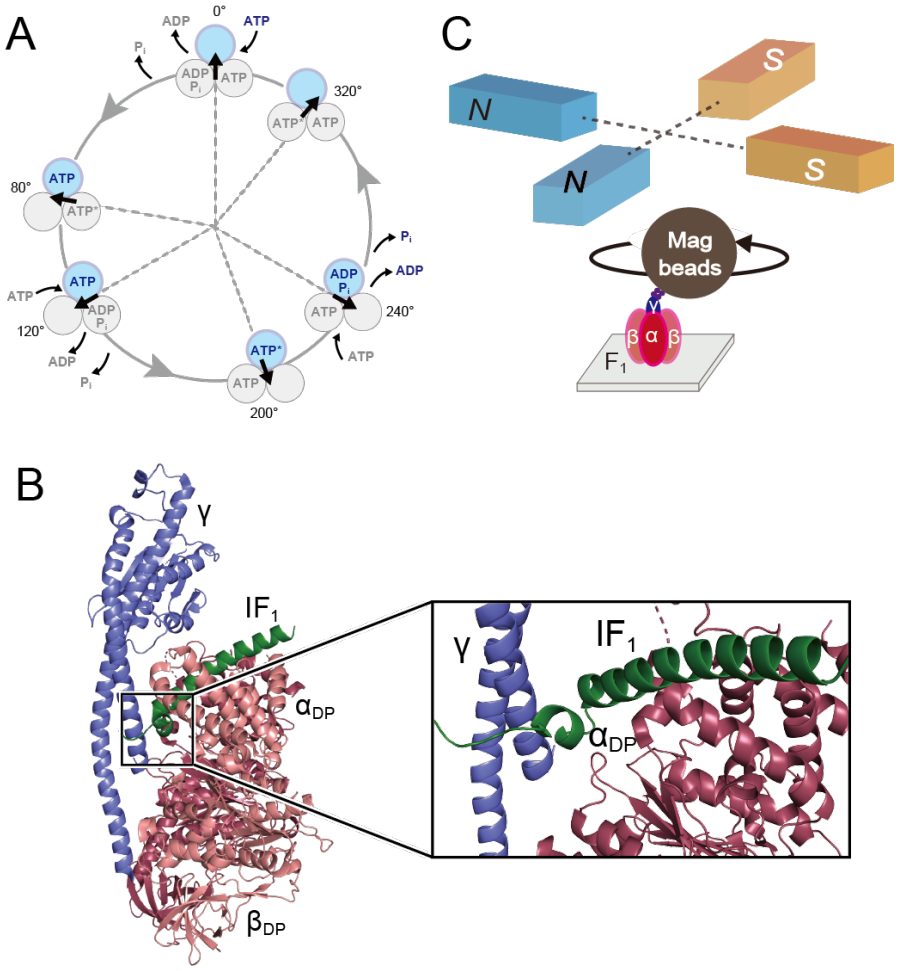

Fig. 1. Outline of this work.

(A) Rotation scheme of *b*MF$_1$. Circles represent the catalytic states of bound nucleotides at β subunit. ATP* in the circles at 80°, 200°, and 320° represents the catalytically active state where the bound ATP is to be hydrolyzed. Arrows represent the rotary angles of γ subunit. 0° is defined as the position of the γ subunit where the blue β subunit binds to ATP. *Short pauses* at 10°-20°, 130°-140°, and 250°-260°, observed in our previous paper [20], are omitted from this figure for clarity.

(B) Crystal structure of *b*MF$_1$ with IF$_1$ bound to the $\alpha\beta_{DP}$ subunit (PDB: 2v7q). α_{DP}, β_{DP}, γ and IF$_1$ are colored by dark red, pink blue, and green, respectively. β_{DP} subunit is omitted for clarity in the enlarged illustration.

(C) An illustration of the single-molecule rotation assay system of *b*MF$_1$. The stator $\alpha_3\beta_3$-ring is immobilized onto a glass surface. A magnetic bead ($\varphi \sim 300$ nm) is attached to the rotor γ subunit as a rotation probe through biotin-streptavidin interaction. Magnetic tweezers, comprising of two sets of electromagnets, were equipped onto the sample stage of the microscope.

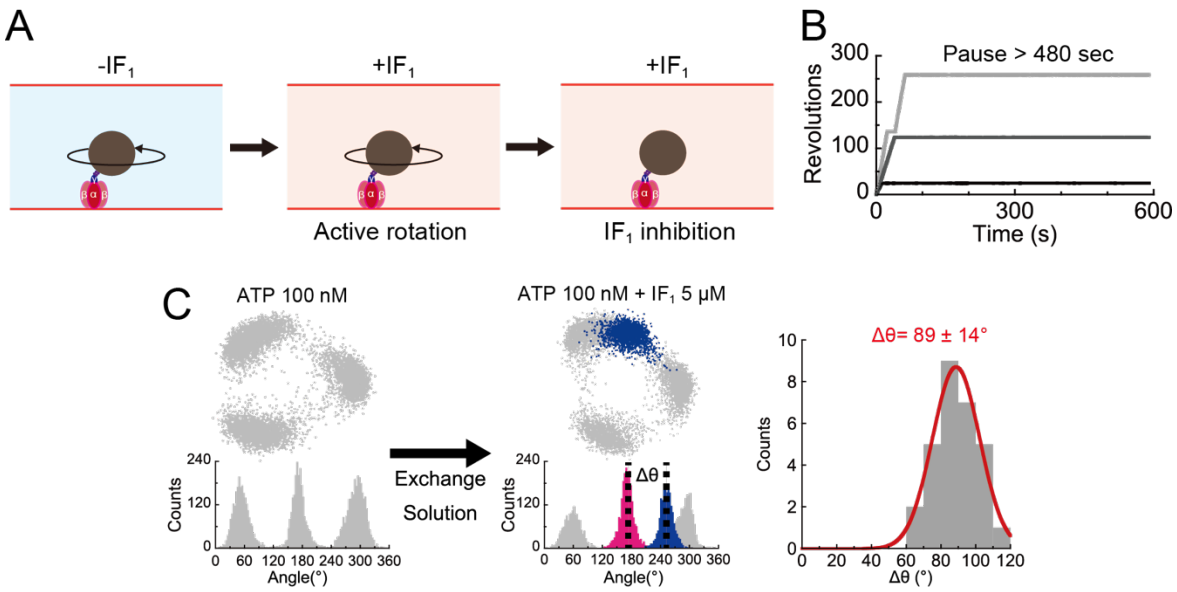

Fig. 2. Single-molecule analysis of IF_1-inhibited *b*MF_1.

(A) Experimental method. After observing a rotating *b*MF_1 molecule in IF_1-free solution, we introduced a mixture solution with IF_1 into the reaction chamber. The *b*MF_1 continued to rotate for a while but finally stops rotation.

(B) Typical time-courses of *b*MF_1 in the presence of 3 μM IF_1 and 1 mM ATP. For more detailed analysis, see Fig. S2.

(C) Stall positions of IF_1 inhibition. (*Left*) An example of the IF_1 inhibited pauses. After observing the ATP-binding waiting dwell at 100 nM ATP, 5 μM IF_1 with 100 nM ATP was introduced into the reaction chamber. Blue data points represent stalls of IF_1 inhibition. (*Right*) The angular distance (Δθ) of IF_1-inhibited from the left-side ATP-binding waiting dwell (pink) ($N = 29$ pauses). Values represent mean ± SD estimated from Gaussian fitting of the datapoints.

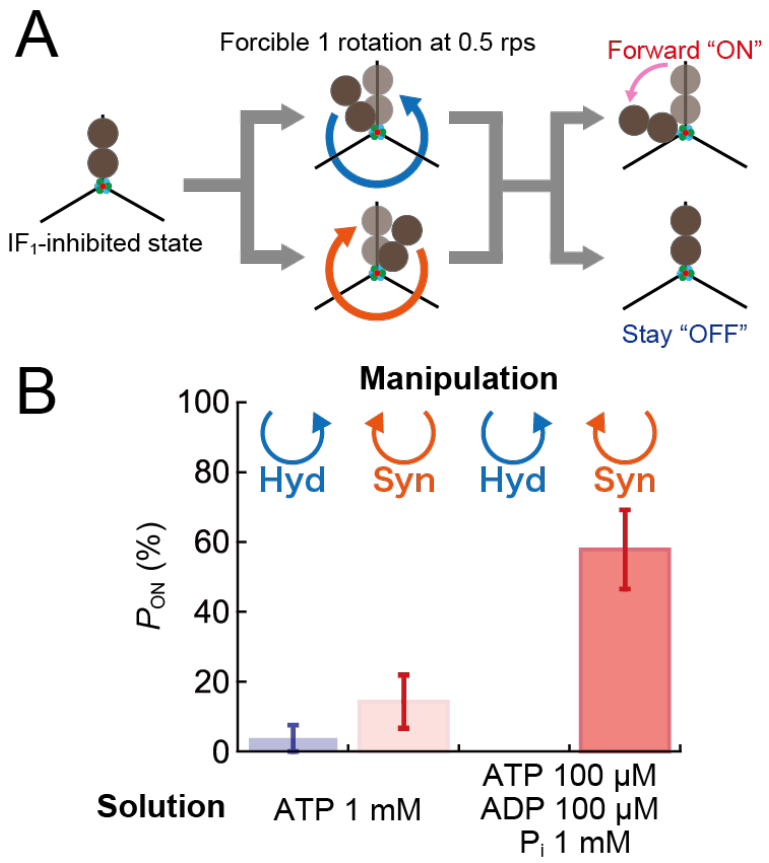

Fig. 3. Single-molecule manipulation of IF$_1$-inhibited *b*MF$_1$.

(A) Schematic images of manipulation procedure. When *b*MF$_1$ was stalled by IF$_1$, the magnetic tweezers were turned on to stall *b*MF$_1$ to rotate one clockwise or counterclockwise revolution at the rate of 0.5 rps. After manipulation, released *b*MF$_1$ either resumed its rotation (ON) or not (OFF). These behaviors indicate whether IF$_1$ is dissociated from *b*MF$_1$ under stalling time or not, respectively.

(B) Reactivation probability of IF$_1$-inhibited *b*MF$_1$ after manipulation. The reactivation probability (P_{ON}) was defined as that of an ON event against total molecules. "Hyd" and "Syn" represent the direction for hydrolysis (counterclockwise) and synthesis (clockwise), respectively. Error bars represent SD, given as $\sqrt{P_{ON}\,(100 - P_{ON})/N}$, where N is the number of total molecules (N = 19-26 molecules).

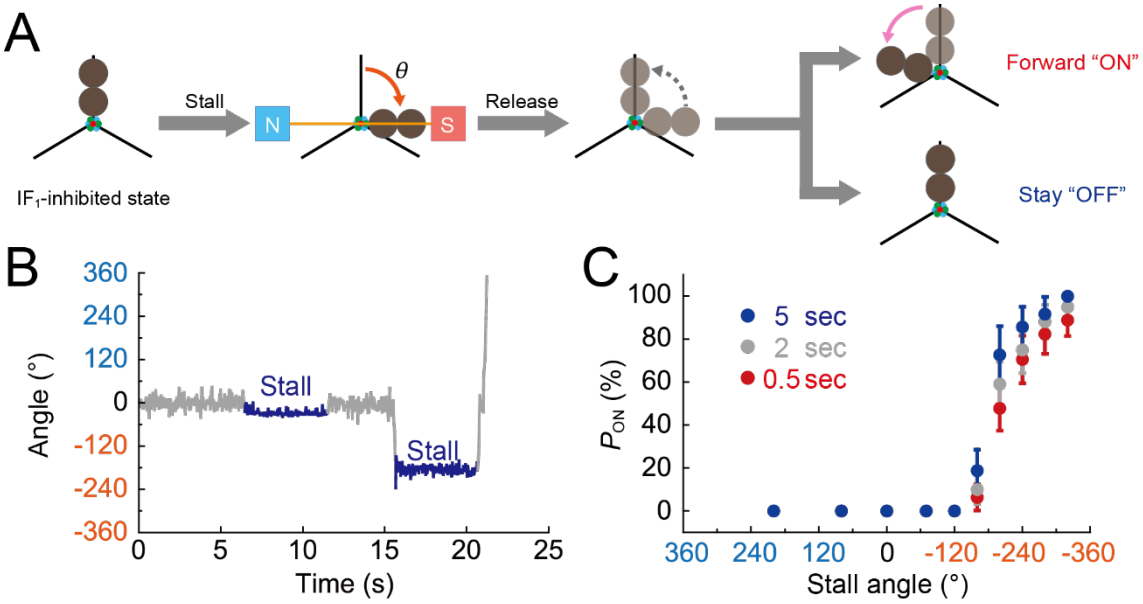

Fig. 4. The stall-and-release experiment of IF_1-stalled *b*MF_1.

(A) Schematic images of manipulation procedure in the stall-and-release experiment. When *b*MF_1 was stalled by IF_1, the magnetic tweezers were turned on to stall *b*MF_1 at the targeted angle. After the set time elapsed, the magnetic tweezers were turned off, and the molecule went back to the initial angle. Released *b*MF_1 either resumes its rotation (ON) or stays at the initial position (OFF). These behaviors indicate whether IF_1 is dissociated from *b*MF_1 under stalling time or not, respectively.

(B) A representative time course of stall-and-release experiment under 100 μM ATP, 100 μM ADP, 1 mM P_i in the presence of 3 μM IF_1. In this figure, the stall time for both trials (blue) was 5 s and the stall angle are -26° and -168°, respectively.

(C) Angle dependence of reactivation probability under 100 μM ATP, 100 μM ADP, 1 mM P_i in the presence of 3 μM IF_1. Each data point was obtained from 15 to 47 trials using 4 to 14 molecules. Counterclockwise rotation (blue) and clockwise rotation (orange) is defined as positive and negative direction, respectively. Colors on the plots represent the stall time of 0.5 s (red), 2 s (grey) and 5 s (blue), respectively. Error bars represent SD, given as $\sqrt{P_{ON}\,(100-P_{ON})/N}$, where N is the number of total trials in each datapoint.

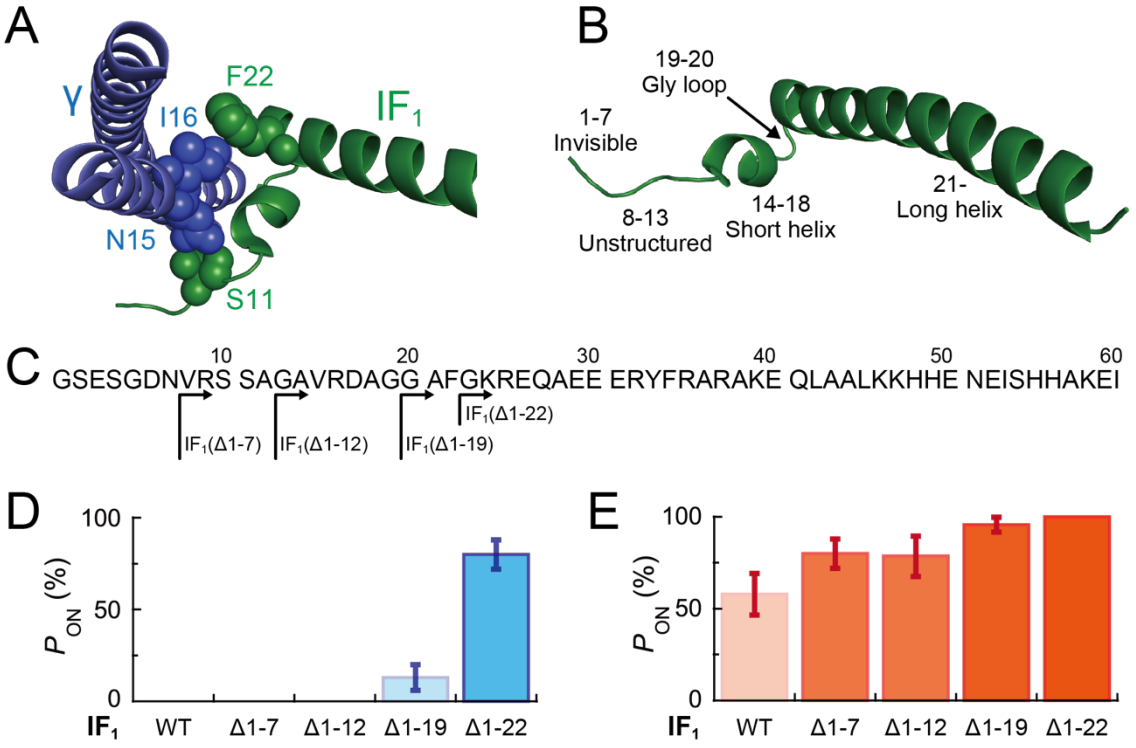

Fig. 5. Analysis of mutant IF$_1$s with N-terminal truncation

(A) Enlarged illustration of interactions between IF$_1$ and γ subunit in the *b*MF$_1$-IF$_1$ complex (PDB: 2v7q). S11 and F22 in IF$_1$ (green) can interact with N15 and I16 in γ subunit (blue), respectively.

(B) Details of IF$_1$ structure (PDB: 2v7q), where residues 8-50 are resolved. Residues 1-7 are not resolved. Residues 8-13 are resolved and form an extended structure. Residues 14-18 and 21-50 form short and long helix, respectively, linked by glycine loop in residues 19-20.

(C) Sequence of bovine IF$_1^{1\text{-}60}$ and definition of N-terminal truncated mutants.

(D) & (E) Reactivation probability of inhibited *b*MF$_1$ by mutant IF$_1$s after (D) counterclockwise and (E) clockwise manipulation. Experiments were conducted under 100 μM ATP, 100 μM ADP, and 1 mM P$_i$. The reactivation probability (P_{ON}) was defined as that of an ON event against total trials. The data for IF$_1$(WT) is the same as Fig. 3*B*. Error bars represent SD, given as $\sqrt{P_{ON}\,(100-P_{ON})/N}$, where N is the number of total molecules (N=11-25 molecules).

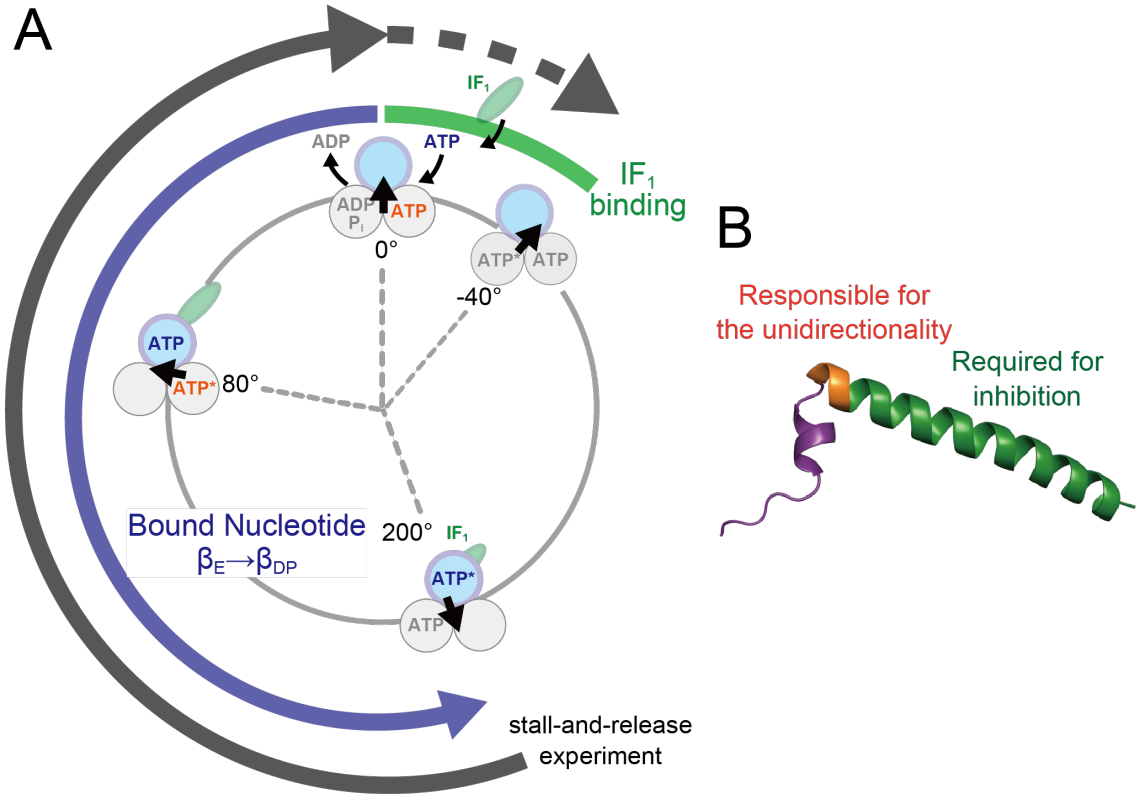

Fig. 6. The proposed mechanisms presented in this study

(A) Coupling scheme of IF_1 dissociation with the rotary mechanism in *b*MF_1. A part of the rotation scheme of *b*MF_1 (Fig. 1A) is described with only the essential elements. The green oval represents IF_1. The green line in the scheme represents the IF_1 binding angle ranging with -40°-0°. The blue line represents the angular difference (0°-200°) required for the conformational transition of the blue β subunit from β_E to β_{DP} via β_{TP}. The black line represents the angle distance for IF_1 dissociation, estimated in the stall-and-release experiment.

(B) The schematic image of the role of IF_1 where residues 8-50 are resolved (PDB: 2v7q). In addition to residues 1-19 (purple), residues 20-22 (orange) are critical for the unidirectionality. Residues from 23 (green) are required for inhibition.

Reference

1. Noji, H., Ueno, H. & McMillan, D. G. G. Catalytic robustness and torque generation of the F1-ATPase. *Biophys Rev* **9**, 103–118 (2017).
2. Junge, W., Lill, H. & Engelbrecht, S. ATP synthase: An electrochemical transducer with rotatory mechanics. *Trends Biochem Sci* **22**, 420–423 (1997).
3. Yoshida, M., Muneyuki, E. & Hisabori, T. ATP synthase - A marvellous rotary engine of the cell. *Nat Rev Mol Cell Biol* **2**, 669–677 (2001).
4. Walker, J. E. E. The ATP synthase: The understood, the uncertain and the unknown. *Biochem Soc Trans* **41**, 1–16 (2013).
5. Kühlbrandt, W. Structure and Mechanisms of F-Type ATP Synthases. (2019) doi:10.1146/annurev-biochem-013118.
6. Xu, T., Pagadala, V. & Mueller, D. M. Understanding structure, function, and mutations in the mitochondrial ATP synthase. *Microbial Cell* **2**, 105–125 (2015).
7. Noji, H., Ueno, H. & Kobayashi, R. Correlation between the numbers of rotation steps in the ATPase and proton-conducting domains of F- and V-ATPases. *Biophys Rev* 303–307 (2020) doi:10.1007/s12551-020-00668-7.
8. Abrahams, J. P., Leslie, A. G. W., Lutter, R. & Walker, J. E. Structure at 2.8 Â resolution of F1-ATPase from bovine heart mitochondria. *Nature* **370**, 621–628 (1994).
9. Cingolani, G. & Duncan, T. M. Structure of the ATP synthase catalytic complex (F1) from Escherichia coli in an autoinhibited conformation. *Nat Struct Mol Biol* **18**, 701–707 (2011).
10. Kabaleeswaran, V., Puri, N., Walker, J. E., Leslie, A. G. W. & Mueller, D. M. Novel features of the rotary catalytic mechanism revealed in the structure of yeast F1 ATPase. *EMBO Journal* **25**, 5433–5442 (2006).
11. Morales-Rios, E., Montgomery, M. G., Leslie, A. G. W. & Walker, J. E. Structure of ATP synthase from Paracoccus denitrificans determined by X-ray crystallography at 4.0 Å resolution. *Proceedings of the National Academy of Sciences* **112**, 13231–13236 (2015).
12. Sobti, M., Ueno, H., Noji, H. & Stewart, A. G. The six steps of the complete F1-ATPase rotary catalytic cycle. *Nat Commun* **12**, (2021).
13. Bowler, M. W., Montgomery, M. G., Leslie, A. G. W. & Walker, J. E. Ground State Structure of F1-ATPase from Bovine Heart Mitochondria at 1.9 Aå Resolution. *Journal of Biological Chemistry* **282**, 14238–14242 (2007).
14. Noji, H. & Ueno, H. How Does F1-ATPase Generate Torque?: Analysis From Cryo-Electron Microscopy and Rotational Catalysis of Thermophilic F1. *Front Microbiol* **13**, (2022).
15. Börsch, M. & Duncan, T. M. Spotlighting motors and controls of single FoF1-ATP synthase. *Biochem Soc Trans* **41**, 1219–1226 (2013).

16. Sielaff, H. & Börsch, M. Twisting and subunit rotation in single FOF1-ATP synthase. *Philosophical Transactions of the Royal Society B: Biological Sciences* vol. 368 Preprint at https://doi.org/10.1098/rstb.2012.0024 (2013).
17. Noji, H., Yasuda, R., Yoshida, M. & Kinosita, K. Direct observation of the rotation of F1-ATPase. *Nature* **386**, 299–302 (1997).
18. Martin, J. L., Ishmukhametov, R., Hornung, T., Ahmad, Z. & Frasch, W. D. Anatomy of F1-ATPase powered rotation. *Proceedings of the National Academy of Sciences* **111**, 3715–3720 (2014).
19. Suzuki, T., Tanaka, K., Wakabayashi, C., Saita, E. & Yoshida, M. Chemomechanical coupling of human mitochondrial F1-ATPase motor. *Nat Chem Biol* **10**, 930–936 (2014).
20. Kobayashi, R., Ueno, H., Li, C.-B. & Noji, H. Rotary catalysis of bovine mitochondrial F1-ATPase studied by single-molecule experiments. *Proceedings of the National Academy of Sciences* **117**, 1447–1456 (2020).
21. Watanabe, R., Iino, R. & Noji, H. Phosphate release in F1-ATPase catalytic cycle follows ADP release. *Nat Chem Biol* **6**, 814–820 (2010).
22. Okuno, D. *et al.* Correlation between the conformational states of F1-ATPase as determined from its crystal structure and single-molecule rotation. *Proc Natl Acad Sci U S A* **105**, 20722–7 (2008).
23. Okazaki, K. I. & Takada, S. Structural comparison of F1-ATPase: Interplay among enzyme structures, catalysis, and rotations. *Structure* **19**, 588–598 (2011).
24. Shimabukuro, K. *et al.* Catalysis and rotation of F1 motor: Cleavage of ATP at the catalytic site occurs in 1 ms before 40 substep rotation. *Proceedings of the National Academy of Sciences* **100**, 14731–14736 (2003).
25. Green, D. W. & Grover, G. J. The IF1 inhibitor protein of the mitochondrial F1F0-ATPase. *Biochimica et Biophysica Acta (BBA) - Bioenergetics* **1458**, 343–355 (2000).
26. Guo, H. *et al.* Structure of mycobacterial ATP synthase bound to the tuberculosis drug bedaquiline. *Nature* **589**, 143–147 (2021).
27. Hahn, A., Vonck, J., Mills, D. J., Meier, T. & Kühlbrandt, W. Structure, mechanism, and regulation of the chloroplast ATP synthase. *Science (1979)* **360**, (2018).
28. Krah, A. Linking structural features from mitochondrial and bacterial F-type ATP synthases to their distinct mechanisms of ATPase inhibition. *Prog Biophys Mol Biol* **119**, 94–102 (2015).
29. Hirono-Hara, Y. *et al.* Pause and rotation of F1-ATPase during catalysis. *Proceedings of the National Academy of Sciences* **98**, 13649–13654 (2001).
30. Hirono-hara, Y., Ishizuka, K., Kinosita, K., Yoshida, M. & Noji, H. Activation of pausing F1 motor by external force. *Proc. Nat. Acad. Sci. USA* **102**, 1–6 (2005).

694 31. Watanabe, R. & Noji, H. Timing of inorganic phosphate release modulates the catalytic
695 activity of ATP-driven rotary motor protein. *Nat Commun* **5**, 3486 (2014).
696 32. Pullman, M. E. & Monroy, G. C. A Naturally Occurring Inhibitor of Mitochondrial
697 Adenosine Triphosphatase. *Journal of Biological Chemistry* **238**, 3762–3769 (1963).
698 33. Saita, E. I. *et al.* Activation and Stiffness of the Inhibited States of F1-ATPase Probed by
699 Single-molecule Manipulation. *Journal of Biological Chemistry* **285**, 11411–11417 (2010).
700 34. Feniouk, B. A., Kato-Yamada, Y., Yoshida, M. & Suzuki, T. Conformational Transitions of
701 Subunit ε in ATP Synthase from Thermophilic Bacillus PS3. *Biophys J* **98**, 434–442 (2010).
702 35. Shah, N. B., Hutcheon, M. L., Haarer, B. K. & Duncan, T. M. F1-ATPase of Escherichia
703 coli. *Journal of Biological Chemistry* **288**, 9383–9395 (2013).
704 36. Xiong, H., Zhang, D. & Vik, S. B. Subunit ε of the Escherichia coli ATP Synthase: Novel
705 Insights into Structure and Function by Analysis of Thirteen Mutant Forms. *Biochemistry* **37**,
706 16423–16429 (1998).
707 37. Schwerzmann, K. & Pedersen, P. L. Regulation of the mitochondrial ATP synthase/ATPase
708 complex. *Arch Biochem Biophys* **250**, 1–18 (1986).
709 38. García-Bermúdez, J. & Cuezva, J. M. The ATPase Inhibitory Factor 1 (IF1): A master
710 regulator of energy metabolism and of cell survival. *Biochim Biophys Acta Bioenerg* **1857**,
711 1167–1182 (2016).
712 39. Esparza-Moltó, P. B. *et al.* Generation of mitochondrial reactive oxygen species is controlled
713 by ATPase inhibitory factor 1 and regulates cognition. *PLoS Biol* **19**, e3001252 (2021).
714 40. Cabezón, E., Montgomery, M. G., Leslie, A. G. W. & Walker, J. E. The structure of bovine
715 F1-ATPase in complex with its regulatory protein IF1. *Nat Struct Mol Biol* **10**, 744–750
716 (2003).
717 41. Bason, J. v, Montgomery, M. G., Leslie, A. G. W. & Walker, J. E. Pathway of binding of the
718 intrinsically disordered mitochondrial inhibitor protein to F1-ATPase. *Proceedings of the*
719 *National Academy of Sciences* **111**, 11305–11310 (2014).
720 42. Gledhill, J. R., Montgomery, M. G., Leslie, A. G. W. & Walker, J. E. How the regulatory
721 protein, IF1, inhibits F1-ATPase from bovine mitochondria. *Proceedings of the National*
722 *Academy of Sciences* **104**, 15671–15676 (2007).
723 43. Cabezón, E., Runswick, M. J., Leslie, A. G. W. & Walker, J. E. The structure of bovine IF1,
724 the regulatory subunit of mitochondrial F-ATPase. *EMBO J* **20**, 6990–6996 (2001).
725 44. van Raaij, M. J. *et al.* The ATPase Inhibitor Protein from Bovine Heart Mitochondria: The
726 Minimal Inhibitory Sequence. *Biochemistry* **35**, 15618–15625 (1996).
727 45. Bason, J. v., Runswick, M. J., Fearnley, I. M. & Walker, J. E. Binding of the Inhibitor
728 Protein IF1 to Bovine F1-ATPase. *J Mol Biol* **406**, 443–453 (2011).

46. Kobayashi, R., Mori, S., Ueno, H. & Noji, H. Kinetic analysis of the inhibition mechanism of bovine mitochondrial F1-ATPase inhibitory protein using biochemical assay. *The Journal of Biochemistry* **170**, 79–87 (2021).
47. Corvest, V. *et al.* The Binding Mechanism of the Yeast F_1-ATPase Inhibitory Peptide: ROLE OF CATALYTIC INTERMEDIATES AND ENZYME TURNOVER *. *Journal of Biological Chemistry* **280**, 9927–9936 (2005).
48. Cintron, N. M., Hullihen, J., Schwerzmann, K. & Pedersen, P. L. Proton-adenosinetriphosphatase complex of rat liver mitochondria: effect of its inhibitory peptide on the ATP hydrolytic and functional activities of the enzyme. *Biochemistry* **21**, 1878–1885 (1982).
49. Hashimoto, T., Negawa, Y. & Tagawa, K. Binding of Intrinsic ATPase Inhibitor to Mitochondrial ATPase—Stoichiometry of Binding of Nucleotides, Inhibitor, and Enzyme. *The Journal of Biochemistry* **90**, 1151–1157 (1981).
50. Gómez-Puyou, A., Tuena de Gómez-Puyou, M. & Ernster, L. Inactive to active transitions of the mitochondrial ATPase complex as controlled by the ATPase inhibitor. *Biochimica et Biophysica Acta (BBA) - Bioenergetics* **547**, 252–257 (1979).
51. Harris, D. A., von Tscharner, V. & Radda, G. K. The ATPase inhibitor protein in oxidative phosphorylation The rate-limiting factor to phosphorylation in submitochondrial particles. *Biochimica et Biophysica Acta (BBA) - Bioenergetics* **548**, 72–84 (1979).
52. Schwerzmann, K. & Pedersen, P. L. Proton-adenosinetriphosphatase complex of rat liver mitochondria: effect of energy state on its interaction with the adenosine triphosphatase inhibitory peptide. *Biochemistry* **20**, 6305–6311 (1981).
53. van de Stadt, R. J., de Boer, B. L. & van Dam, K. The interaction between the mitochondrial ATPase (F1) and the ATPase inhibitor. *Biochimica et Biophysica Acta (BBA) - Bioenergetics* **292**, 338–349 (1973).
54. Klein, G. & Vignais, P. v. Effect of the protonmotive force on ATP-linked processes and mobilization of the bound natural ATPase inhibitor in beef heart submitochondrial particles. *J Bioenerg Biomembr* **15**, 347–362 (1983).
55. Lippe, G., Sorgato, M. C. & Harris, D. A. Kinetics of the release of the mitochondrial inhibitor protein. Correlation with synthesis and hydrolysis of ATP. *Biochimica et Biophysica Acta (BBA) - Bioenergetics* **933**, 1–11 (1988).
56. Watanabe, R. *et al.* Mechanical modulation of catalytic power on F1-ATPase. *Nat Chem Biol* **8**, 86–92 (2012).
57. Milgrom, Ya. M. An ATP dependence of mitochondrial F1-ATPase inactivation by the natural inhibitor protein agrees with the alternating-site binding-change mechanism. *FEBS Lett* **246**, 202–206 (1989).

58. Corvest, V., Sigalat, C. & Haraux, F. Insight into the Bind−Lock Mechanism of the Yeast Mitochondrial ATP Synthase Inhibitory Peptide. *Biochemistry* **46**, 8680–8688 (2007).
59. Mendoza-Hoffmann, F., Zarco-Zavala, M., Ortega, R. & García-Trejo, J. J. Control of rotation of the F1FO-ATP synthase nanomotor by an inhibitory α-helix from unfolded ε or intrinsically disordered ζ and IF1 proteins. *J Bioenerg Biomembr* **50**, 403–424 (2018).
60. García-Trejo, J. J. *et al.* The Inhibitory Mechanism of the ζ Subunit of the F1FO-ATPase Nanomotor of Paracoccus denitrificans and Related α-Proteobacteria*. *Journal of Biological Chemistry* **291**, 538–546 (2016).
61. Zarco-Zavala, M. *et al.* The 3 × 120° rotary mechanism of Paracoccus denitrificans F1-ATPase is different from that of the bacterial and mitochondrial F1-ATPases. *Proceedings of the National Academy of Sciences* 202003163 (2020) doi:10.1073/pnas.2003163117.
62. Chui-Fann, W. & Gerhard, G. The Unique C-Terminal Extension of Mycobacterial F-ATP Synthase Subunit α Is the Major Contributor to Its Latent ATP Hydrolysis Activity. *Antimicrob Agents Chemother* **64**, e01568-20 (2020).
63. Harikishore, A. *et al.* Targeting Mycobacterial F-ATP Synthase C-Terminal α Subunit Interaction Motif on Rotary Subunit γ. *Antibiotics* **10**, 1456 (2021).
64. Montgomery, M. G., Petri, J., Spikes, T. E. & Walker, J. E. Structure of the ATP synthase from Mycobacterium smegmatis provides targets for treating tuberculosis. *Proceedings of the National Academy of Sciences* **118**, e2111899118 (2021).
65. Andrianaivomananjaona, T., Moune-Dimala, M., Herga, S., David, V. & Haraux, F. How the N-terminal extremity of Saccharomyces cerevisiae IF1 interacts with ATP synthase: A kinetic approach. *Biochimica et Biophysica Acta (BBA) - Bioenergetics* **1807**, 197–204 (2011).
66. Ma, J. *et al.* A Dynamic Analysis of the Rotation Mechanism for Conformational Change in F1-ATPase. *Structure* **10**, 921–931 (2002).
67. Watanabe, R., Hayashi, K., Ueno, H. & Noji, H. Catalysis-Enhancement via Rotary Fluctuation of F1-ATPase. *Biophys J* **105**, 2385–2391 (2013).

Response to Reviewer comments [NCOMMS-22-41840]

We sincerely appreciate the Reviewers for their careful reading and constructive comments. According to the comments, we have revised the manuscript. A step-by-step response is provided below (reviewer comments in *green* and our replies in black).

Reviewer #1

The manuscript "Molecular mechanism on forcible ejection of ATPase inhibitory factor 1 from mitochondrial ATP synthase" by Kobayashi et al. reports new and interesting findings concerning the interactions of regulatory protein IF1 and F1-subcomplex of bovine mitochondrial ATP synthase. The authors used proteins heterologically expressed in Escherichia coli. The ATPase activity of F1-subcomplex was measured both by biochemical methods and by single-molecule assay when it was immobilized on a glass and a bead was attached to subunit gamma, so that in responce to addition of ATP the authors could directly observe bead rotation. The latter method is a very powerful technique that allows to analyze enzyme activity and it regulation in molecular details.

The authors found that IF1 is a very efficient inhibitor of F1 ATPase activity. At temperature of 23C it bound to F1 with a time constant of 20 s at ATP concentration of 1 mM. This finding suggests that IF1 might promptly block ATP hydrolysis by FoF1 in mitochondria under de-energized conditions. The authors also demonstrated that IF1-inhibited F1 can be re-activated by forced rotation of subunit gamma in the ATP synthesis direction, but not in the hydrolysis direction. This is a new and important finding; previous studies of two other common regulatory mechanisms of bacterial F1 (ADP-inhibition and subunit epsilon) demonstrated activation in response to forced rotation in both directions. Finally, by using mutated variants of IF1 (with N-terminal truncations of 7, 12, 19, and 22 amino acid residues) the authors established that the interaction of N-terminal region of IF1 with subunit gamma is important for stabilization of the IF1-inihbited state of F1.

The manuscript is well-written in good English, the logic is clear, the methods are described in sufficient details, and the results support the conclusions. I think the manuscript can be published in Nature Communications after solving some issues described below.

We thank the reviewer for taking the time for reviewing and giving helpful comments. We revised the manuscript along the comments as below.

(1) All the experiments were done at 23C, while the physiological temperature for a cow is about 37C; at 23C body temperature a cow is kind of dead. It is clear that repeating the single-molecule experiments at 37C is not an option (lots of work + technically challenging), but it is possible to repeat the biochemical activity measurements and the effects of IF1 at 37C. ATP synthase regulatory mechanisms are known to be temperature-dependent, so demonstrating that 23C and 37C experiments provide qualitatively similar results it important.

Along the comment, we conducted biochemical analysis of the representative mutant IF_1s $IF_1(\Delta 1\text{-}19)$ and $IF_1(\Delta 1\text{-}22)$ and the wild-type, IF_1(WT) to confirm that fundamental aspects are observed at more physiological condition, at 37ºC. We show below the time course of inhibition

(left; 25ºC, center; 37ºC, in (A), (C), (E)) and the resulting residual ATPase activity (right, in (B), (D), (F)). The result at 37ºC was essentially identical to that at 25ºC, as seen in the original manuscript: IF_1(WT) showed complete inhibition with no residual activity, whereas IF_1(Δ1-19) and IF_1(Δ1-22) did not completely inhibit ATPase activity. We also found that the efficiency of IF_1 inhibition at 37ºC was about five-fold lower than that at 25ºC. This observation was well consistent with the previous finding that the chemical equilibrium between inhibition and dissociation in IF_1 kinetics is shifted to dissociation when temperature increases (Fergunson, *et al*., *Biochem. J*. 1977).

In summary, our biochemical experiment suggests that the principle of IF_1 inhibition and dissociation is preserved between at room temperature and at physiological temperatures of mitochondria, 37ºC, supporting the generality of the findings in the present study. We have revised the *Discussion* (line 330-338), providing the figure of this experimental result to Supplementary Fig. 13 and 14.

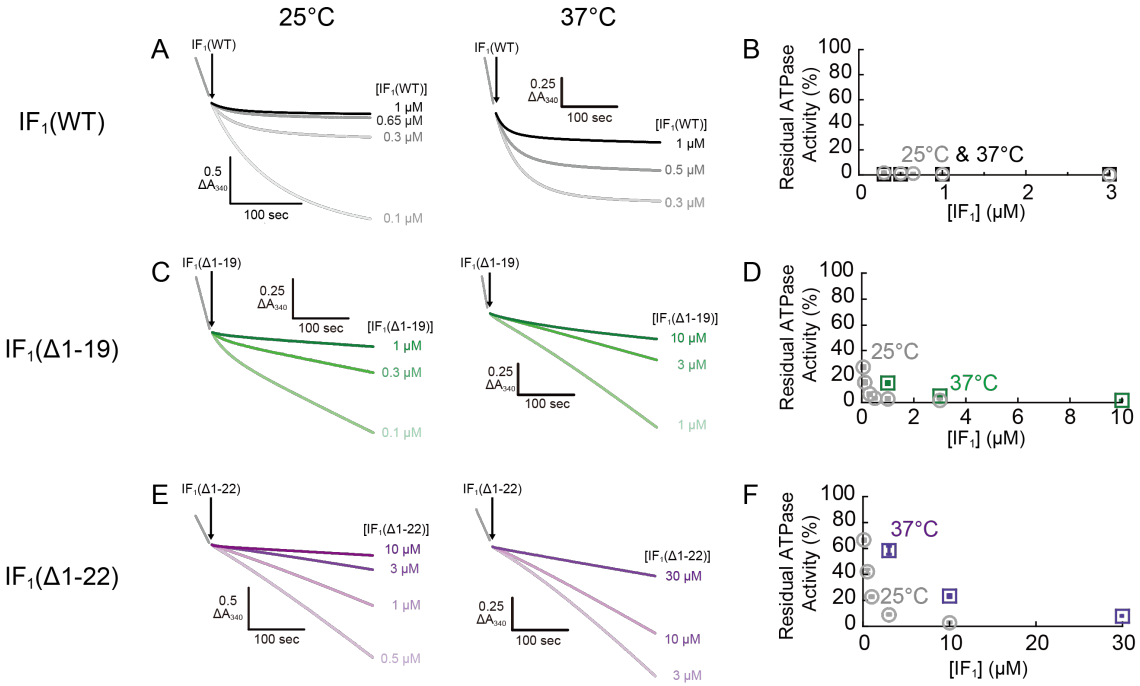

Figure. Biochemical analysis under 37°C.

(A, C, E) Time courses for IF_1-inhibited *b*MF_1 at 25°C and 37°C with the indicated concentrations of (A) IF_1(WT) (black/gray), (C) IF_1(Δ1-19) (green), (E) IF_1(Δ1-22) (purple). (B, D, F) Residual ATPase activity versus [IF_1] at the end of the measurement (350 s after IF_1 injection). Colored squares (black, green, purple) represent results at 37°C and gray circles represent results at 25°C (shown in Supplementary Fig. 8), respectively. Symbols and error bars represent the mean value and SD, respectively (N = 3 for each measurement).

(2) It was shown for Bacillus PS3 F1 (Ref. 34) that activation by forced rotation from ADP-inhibited state and from epsilon-inhibited state requires more energy than ATP synthesis. Is it possible to estimate, whether this is also the case with IF1 inhibition of bovine F1? This is a very important issue, because it affects the pattern of activation in whole mitochondria, where many copies of ATP synthase share the same coupling membrane. It might also explain why some research groups observed the decrease in ATP synthesis rate upon IF1 association to FoF1.

This is an interesting and important question from mechanistic and energetic point of view. However, this study does not quantify the torque at which magnetic tweezers exert F_1. Therefore, it is not possible to directly estimate the minimum membrane voltage for the injection of IF_1. However, when *b*MF_1 generates torque of 40 pN·nm like other F_1s, the minimum value for proton motive force as voltage to reverse F_1 is 196 mV, considering the proton stoichiometry of 8 protons/turn. In addition, the minimum energy for IF_1 ejection is assumed to be 140 pN·nm (84 kJ/mol). Although these estimations are tentative, we provide this discussion in the revised manuscript (line 295-300).

(3) It is stated in the text (lines 179-181) that some molecules were excluded from the analysis. Since single-molecule assays provide the researcher with an option to choose "good" molecules and ignore "bad" ones, it would be nice to include a table (in Supporting materials) that provides some statistics, e.g. how many molecules were in the view field of the microscope, how many of them were totally inactive, how many of the active ones were later rejected from the analysis.

Along this comment, we have added a table about information in the single-molecule experiment to Supplementary Table 6.

(4) The authors provide time constants for rotation phase and inhibition phase. However, for a biochemist it is more important to know, what percentage of time F1 was active, and what percentage of time it was inactive. (It can be calculated from the time constants, but it is not quite simple). I suggest that the information on the fractions of time that the enzyme was active/inactive should be added to the results section.

Thank you for your suggestions. Along this, we provide tables for comparison of active/inactive states to Supplementary Table 4 and 5. For biochemical measurements of IF_1 inhibition, readers can obtain similar information from the 'Residual ATPase Activity versus [IF_1]' shown in the Supplementary Figure 8 and 10.

- *Minor comment*

(5) Line 34 - "counterclockwise" is ambiguous, until the reader knows from which side we are looking

Thank you for the advice. Along this comment, we added the description of 'when viewed from the membrane side' in the corresponding part.

(6) Line 40 - "rotated" is kind of confusing here, because rotation is generally associated with the rotor rotation. May be use the term "swing-out motion" as in line 278?

We have revised the corresponding part along the suggestion.

(7) *Line 46 - ATP synthesis is the primary role of FoF1 in mitochondria, but not in many bacteria. Better to specify it.*

Thank you for the constructive comment. Along this, we revised the manuscript to notify readers of this contention.

(8) *Line 53 - I have not seen any data direct on the effect of pmf on IF1 association. In bovine mitochondria pH is a crucial factor that controls IF1 association, and I strongly recommend to add this fact to the Introduction. Acidification of the matrix usually results from anoxia and is accompanied by the drop in pmf, but it is difficult to prove the causal link between pmf and IF1 association.*

Thank you for your careful reading. Along this suggestion, we have revised the manuscript.

(9) *Line 140 - what was the concentration of ATP?*

Along the comment, we added the description for the exact ATP concentration (1 mM) in the revised manuscript.

(10) *Line 268 - the authors demonstrated that Pi also increases the probability of IF1 release upon gamma rotation, so ADP is not critically important for that. The discussion should be corrected accordingly.*

Thank you for the constructive comment. Along this, we have revised the manuscript.

(11) *Lines 342-347 - I think that the data on alanine substitutions are interesting and informative; may be include them in the results section?*

Along this suggestion, we provide the additional data and information on alanine substitutions as Supplementary text and Supplementary Fig. 11.

(12) *Finally, citing some recent reviews on the regulatory mechanisms of ATP synthase might also improve the manuscript.*

Along this comment, we added the recent review papers on regulation of ATP synthase (Cheuk A and Meier T, *Biochem. Soc. Trans*. 2021; Mendoza-Hoffmann F, *et al*., *Microorganisms*. 2022) in adequate places in the revised manuscript (No. 29 & 30 with new numbering).

- *Additional comments shown in the attached pdf file*

(13) *Line 44 – 'Bacillus' should be italic*

(14) *Line 51 – Should add 'is' before 'highly'*

(15) *Line 79 – Remove the 'it' before F_1 (same as the comment (21)).*

(16) *Line 337 – 'requisite' may be replaced with 'required'*

We appreciate his/her careful reading of the manuscript. Along these comments, we have

revised the manuscript.

(17) Line 98 – What is "φ"?

'φ' is a diameter of the magnetic beads used in this work. To avoid misunderstanding, we added the words 'beads diameter' before 'φ' in the revised manuscript.

(18) Line 173 – 'false' may be replaced with 'inability' or 'fail'

Along this comment, we have replaced 'false' with 'failure'.

Reviewer #2

The manuscript demonstrates the mechanism of release of the inhibitor IF1 from ATP-synthase, using magnetic tweezers to mimic and assist ATP synthesis. Technically it is exemplary, the conclusions are demonstrated beautifully, clearly, and beyond doubt using a method that while not novel remains extremely challenging. I am not qualified to judge the significance of the result to the field of inhibitory control of ATP synthase. From the perspective of single-molecule biology, it is of great interest to a general reader as an example of the use of single molecule methods to reveal mechanistic details in biological molecular machines.

We sincerely appreciate the high evaluation by the Reviewer 2.

Reviewer #3

This study reports single-molecule manipulation experiments with immobilized bovine F1 linked to magnetic beads to elucidate the molecular mechanism of F1 inhibition by its natural inhibitory peptide IF1. The results showed that IF1-inhibited F1 was efficiently activated only when F1 was forcibly rotated (with magnetic tweezers) in the clockwise (ATP synthesis) direction, but not in the counter-clockwise direction (ATP hydrolysis), and the activation was enhanced in the presence of ADP and Pi. These observations suggest that the principal mechanism for the pmf-induced activation of IF1-inhibited FoF1 (in membranes) is the ejection of IF1 from F1 by pmf-driven Fo motor rotation. The results obtained with IF1 mutants strongly support a model in which the inhibitory effect of IF1 is mainly due the prevention of subunit beta conformational changes rather than changes in the interactions of IF1 with subunit gamma. These are major findings that provide novel and important insights into the mechanisms that regulate the activity of F1FO complexes. The presentation of the work is excellent.

We are most grateful for this reviewers' positive and encouraging comments on the work and are delighted to add the additional information requested.

- *Minor comment*

(19) In the introduction (lines 52, 53), the authors may want to include a previous reference (Lefebvre-Legendre et al. Mol. Microbiol 2003) showing that F1-mediated ATP hydrolysis is essential for cell viability, for instance in cells of Saccharomyces cerevisiae lacking functional mitochondrial DNA (and hence the FO) where this activity is absolutely needed to maintain a sufficient mitochondrial membrane potential by the ADP/ATP translocase. In these pure ATP hydrolysis conditions, inhibition of F1 by IF1 would be lethal rising the possibility that IF1 does not necessarily bind to the F1 when it cannot dock to FO?

Thank you for the careful reading and comments. The original manuscript attempted to mean that the hydrolysis activity of isolated F_1 before assembling onto F_o, but not ATP hydrolysis coupled with proton pumping for membrane voltage maintenance. To clarify this point, we revised the manuscript (line 55-56).

(20) The formulation "activation of IF1 inhibition" used all along the manuscript to indicate that F1 inhibition by IF1 is released is a bit confusing because it suggests instead that F1 becomes inhibited by IF1.

We appreciate the comment. To avoid misunderstandings, we define the meaning of "activation of/from IF_1 inhibition" as "IF_1 ejection from the catalytic site of F_1 and the recovery of catalysis in F_1" in the first place of the revised manuscript (line 84).

(21) line 79. Remove the 'it' before F1 (same as the comment (15)).

Along this comment, we removed the corresponding 'it'.